



HAL
open science

A model for tropospheric multiphase chemistry: application to one cloudy event during the CIME experiment

Maud Leriche, Didier Voisin, Nadine Chaumerliac, Anne Monod, Bernard
Aumont

► To cite this version:

Maud Leriche, Didier Voisin, Nadine Chaumerliac, Anne Monod, Bernard Aumont. A model for tropospheric multiphase chemistry: application to one cloudy event during the CIME experiment. *Atmospheric Environment*, 2000, 34 (29-30), pp.5015-5036. 10.1016/S1352-2310(00)00329-0. hal-01819409

HAL Id: hal-01819409

<https://uca.hal.science/hal-01819409>

Submitted on 1 Sep 2022

HAL is a multi-disciplinary open access archive for the deposit and dissemination of scientific research documents, whether they are published or not. The documents may come from teaching and research institutions in France or abroad, or from public or private research centers.

L'archive ouverte pluridisciplinaire **HAL**, est destinée au dépôt et à la diffusion de documents scientifiques de niveau recherche, publiés ou non, émanant des établissements d'enseignement et de recherche français ou étrangers, des laboratoires publics ou privés.



Distributed under a Creative Commons Attribution - NonCommercial - NoDerivatives 4.0
International License

A model for tropospheric multiphase chemistry: application to one cloudy event during the CIME experiment

Maud Leriche^{a,*}, Didier Voisin^b, Nadine Chaumerliac^a,
Anne Monod^c, Bernard Aumont^d

^aLaboratoire de Météorologie Physique (LaMP), Université Blaise Pascal, 24 av. des Landais, 63177 Aubière, Cedex, France

^bLaboratoire de Glaciologie et Géophysique de l'Environnement du CNRS (LGGE), BP 96, 38402 Saint Martin d'Hères, Cedex, France

^cLaboratoire de Chimie et Environnement (LCE), Université de Provence, 3 place Victor Hugo, 13003 Marseille, France

^dLaboratoire Interuniversitaire des Systèmes Atmosphériques (LISA), Université Paris 7-Paris 12, Faculté des Sciences, 61 av. du Gal de Gaulle, 94010 Créteil, Cedex, France

A multiphase box model for a remote environment of the troposphere has been developed with an explicit chemistry for both gas and aqueous phase. The model applied to a set of measurements performed by Voisin et al. (2000) during the European CIME experiment for a cloud event on 13th December 1997 at the top of the Puy de Dôme (France). The results of the simulation are compared to the measurements in order to follow the evolution of the ambient chemical composition as a function of the pH and of the varying water content. After verifying that the model retrieves the main features observed in the behavior of species in the cloud droplets, a detailed analysis of the simulated chemical regime is performed. It essentially discusses the sources and sinks of radical in aqueous phase, the relative importance of the oxidation pathways of volatile organic compounds by the main radicals and the conversion of S(IV) into S(VI) which seems to be influenced by the presence of peroxyoxynitric acid, HNO₄, in aqueous phase in the environmental conditions that are considered with low H₂O₂. These numerical results are then compared with the theoretical study from Herrmann et al. (2000), who proposed a slightly different mechanism, including C₂ chemistry and transition metal chemistry whereas they neglect some reaction pathways, such as the one involving OHCH₂O₂ radical. This double confrontation between model results and both real experimental data and numerical results from Herrmann et al. (2000) underlines limitations of such modeling approach that does not include any dynamical or microphysical coupling but also demonstrates its capability to identify the main oxidants or reactants in aqueous phase in real environmental conditions more realistic than a purely theoretical approach. The originality of this study resides in the explicit and exhaustive ways the chemical reactions are treated in aqueous phase and in a first attempt to compare such a detailed chemical scheme to real environmental conditions.

Keywords: Aqueous-phase photochemistry; CIME; Numerical simulation; Deviation from Henry's law

1. Introduction

Tropospheric multiphase chemistry is still poorly understood, because the interactions between trace gases

and the condensed phase are quite complex (Ravishankara, 1997). Clouds can interact with the tropospheric chemistry through different processes. They can remove gaseous species dissolved in the droplets by sedimentation or they can detrain them at various altitudes. Clouds can modify the actinic flux and the photochemistry is, then, more intense around the cloud top and less intense below (Madronich, 1987; Madronich and Flocke, 1999). After their evaporation, clouds modify trace gas

* Corresponding author. Tel.: + 33-4-73-40-73-67; fax: + 33-4-73-40-51-36.

E-mail address: leriche@opgc.univ-bpclermont.fr (M. Leriche).

composition of the troposphere (Huret et al., 1994). Clouds can also indirectly perturb the gas-phase chemistry through the uptake of soluble gases by cloud droplets and ice crystals, through aqueous chemical reactions (see for example, Lelievre and Crutzen, 1991) and through microphysical redistribution (Grégoire et al., 1994).

There are two reasons for the lack of knowledge concerning such complex interactions. First, simultaneous chemical measurements in both gas and aqueous phase are difficult. Usually, the measurements provide integrated results over several 10 minutes especially in cloud water (see for examples: Richards, 1995; Jaeschke et al., 1998; Collett et al., 1990) and do not provide detailed time-resolved information about the scavenging process. Sometimes, only rainwater concentrations are available and cloud water composition is not at all documented (Kieber et al., 1999; Losno et al., 1998). Recent continuous measurements done with a CVI (counterflow virtual impactor) (Noone et al., 1988) introduce biases due to its principle of separating cloud phases. So, there are still a number of problems of chemical measurements in cloud phases (interstitial air, cloud water and particulate). The second problem is that multiphase model validation is still very limited due to the lack and the uncertainties in in situ measurements. Sophisticated models often use theoretical scenarios rather than observations (Bott, 1999; Herrmann et al., 2000). Others are considering size-resolved cloud chemistry but most of the time limit their study to rather simple chemistry (Colville et al., 1994; Wells et al., 1997). Nevertheless, those models need to be applied for studying processes and interactions and for supporting the interpretation of the multiphase measurements.

Our aim in this paper is not to achieve a strict comparison between model and observations but only to retrieve orders of magnitude and tendencies in the behavior of the species with respect to liquid water content. A close comparison is not possible for two reasons: first, the chemical model does not simulate renewal of the atmospheric gases into the cloud through any dynamical or microphysical processes; secondly, data represent integrated measurements of aqueous-phase concentrations over 15–30 min periods of time. Also, this chemical model has been developed with the final aim of coupling it with an air parcel model including microphysics. Results presented here represent a first attempt to this coupling by considering real observational data to calibrate the chemistry as a function of a varying water content which evolves over three hours.

In this study, we present a box model for tropospheric multiphase chemistry that is based on an explicit chemical mechanism in both gas and aqueous phase. This model has been used for the modeling of a cloud event that was documented by the multiphase measurements performed by Voisin et al. (2000) during the European

CIME (cloud ice mountain experiment) experiment. After describing the multiphase chemical box model with its detailed mathematical formulations, we present evolutions of the pH and some species as a function of the liquid water content and compare them with the observed evolutions found by Voisin et al. (2000). Since measurements of the droplet radius were not available on that day, we look at the sensitivity of the gas-phase production rates of the HO₂ radical to different droplet radius. Then, focusing on a particular event of the CIME experiment, a detailed analysis of the cloud chemical regime is presented with special emphasis on radical chemistry and on S(IV) to S(VI) conversion. In addition, by using theoretical recent results from Herrmann et al. (2000), we examine the sensitivity of some volatile organic compounds oxidation pathways by radicals to the variable liquid water content.

2. Description of the multiphase box model

The model is based on a chemical box model developed by Madronich and Calvert (1990) for the gas phase, and includes an automated writing of the chemical mechanism code. For solving the set of chemical equations, two choices of chemical solvers are available: the Gear's solver (Gear, 1971) or the QSSA VTS solver developed by Audiffren et al. (1998). The model can use time series of temperature, density, concentration of water vapor, NO_x and ozone, liquid water content, radius of droplets and photolysis coefficients.

2.1. Chemical mechanisms

The gaseous mechanism is the same than in the original code of Madronich and Calvert (1990). This chemical mechanism is explicit and can be adapted for any environment in the troposphere. In the present study, the gaseous mechanism has been adapted to a rural environment, which includes 101 reactions and 48 gaseous species describing the chemistry of methane, sulfur, NO_y and ammonia.

The initial model has been extended to include the exchange of chemical species between gas and aqueous phases of the cloud (Audiffren et al., 1998), which is parameterized by the mass transfer kinetic formulation developed by Schwartz (1986). We include also the possibility of estimating unknown Henry's law constants for COV (volatile organic compounds) according to the parameterization developed by Suzuki et al. (1992) and adapted by Aumont et al. (1999). The thermodynamical data that are involved in the mass transfer kinetics are listed in Table 1 for accommodation coefficients and Henry's law constants and in Table 2 for aqueous-phase equilibrium. All accommodation coefficients for which there are no measurement are set equal to 0.05 as in

Table 1
Values of mass accommodation coefficients and Henry's law constants

Species	α	H_{298} (M atm ⁻¹)	$\Delta H/R$ (K)
O ₃	0.05 ^a	1.1×10^{-2b}	- 2300 ^b
O ₂	0.05 (estimated)	1.3×10^{-3c}	- 1500 ^c
H ₂ O ₂	0.11 ^d	8.33×10^{4e}	- 7400 ^e
HO ₂	0.2 ^f	4.103 ^f	- 5900 ^f
OH	0.05 (estimated)	30 ^f	- 4500 ^f
NO	0.0001 ^g	1.9×10^{-3c}	- 1400 ^c
NO ₂	0.0015 ^h	1.2×10^{-2i}	- 2500 ⁱ
NO ₃	0.0025 ^j	6.10^{-1k}	
N ₂ O ₅	0.0037 ^l	2.1 ^m	- 3400 ^m
HNO ₂	0.05 ⁿ	50 ^o	- 4900 ^o
HNO ₃	0.054 ^d	2.1×10^{5p}	- 8700 ^p
HNO ₄	0.05 (estimated)	1.2×10^{4q}	- 6900 ^q
NH ₃	0.04 ^r	61 ^s	- 4200 ^s
HCl	0.064 ^d	1.1 ^t	- 2000 ^t
SO ₂	0.11 ^u	1.4 ^v	- 2900 ^v
H ₂ SO ₄	0.07 ^d	$2.1 \times 10^5 = H_{\text{HNO}_3}$	- 8700 = ΔH_{HNO_3}
CO ₂	0.0002 ^v	3.6×10^{-2w}	- 2200 ^w
CH ₃ O ₂	0.05 (estimated)	15 ^x	- 3700 ^x
OHCH ₂ O ₂	0.05 (estimated)	8.05×10^{4x}	- 8200 ^x
CH ₂ O	0.02 ^y	3.10 ^{3z}	- 7200 ^z
HCOOH	0.012 ^d	8.9×10^{3aa}	- 6100 ^{aa}
CH ₃ OOH	0.0038 ^d	3.11×10^{2c}	- 5200 ^c
OHCH ₂ OOH	0.05 (estimated)	1.7×10^{6c}	- 9700 ^c
CH ₃ OH	0.015 ^d	2.2×10^{2ab}	- 5200 ^{ab}
CH ₂ (OH)(OH)	0.05 (estimated)	1.21×10^{7ac}	
CH ₃ (ONO ₂)	0.05 (estimated)	2 ^{ad}	- 4700 ^{ad}

^aMagi et al. (1996).

^bKosak-Channing and Helz (1983).

^cLide and Frederikse (1995).

^dDavidovits et al. (1995).

^eO'Sullivan et al. (1996).

^fHanson et al. (1992).

^gSaastad et al. (1993).

^hPonche et al. (1993).

ⁱNBS (1965).

^jMihelcic et al. (1993).

^kRudich et al. (1996).

^lGeorge et al. (1994).

^mFried et al. (1994).

ⁿBongartz et al. (1994).

^oBecker et al. (1996).

^pSchwartz and White (1981).

^qRégimbal and Mozurkewich (1997).

^rBongartz et al. (1995).

^sClegg and Brimblecombe (1989).

^tMarsh and McElroy (1985).

^uWorsnop et al. (1989).

^vSchurath et al. (1996).

^wZheng et al. (1997).

^xestimated from the empirical relation: $H_{\text{RO}_2} = (H_{\text{ROOH}} * H_{\text{HO}_2}) / H_{\text{H}_2\text{O}_2}$.

^yJayne et al. (1991).

^zBetterton and Hoffmann (1988a).

^{aa}Johnson et al. (1996).

^{ab}Snider and Dawson (1985).

^{ac}estimated from: Suzuki et al. (1994).

^{ad}Kames and Schurath (1992).

Lelieveld and Crutzen (1991). All species scavenged in the droplets react except CH₂(OH)(OH) and CH₃(ONO₂) for which no data are available on their reactivities in aqueous phase and for which gas-phase concentrations are small, respectively, 10⁻¹⁴ and 10⁻⁵ ppbv.

The chemical mechanism in aqueous phase is completely explicit with detailed chemistry of HO_x (Table 3), of chlorine (Table 4), of carbonate (Table 5), of N-species (Table 6), of organic species with one carbon atom (Table 7) and of S-species (Table 8). 156 aqueous-phase reactions and 42 aqueous-phase species are used in this

mechanism based upon the work of Jacob (1986). It then has been updated with the latest kinetics and thermodynamic laboratory data available and with the work of Herrmann et al. (1999a, 2000). HO_x, chlorine, carbonate, N- and S-species chemistry are almost the same as in the mechanism presented by Herrmann et al. (1999a, 2000) with however some differences (reactions A1, A8, A20, A25, A26, A37, A48, A52, A61, A65, A66, A69, A149 are not taken into account in Herrmann et al., 1999a, 2000). For organic species, Herrmann et al. (1999a, 2000) do not take into account cross reactions of RO₂ radical (R = H,

Table 2
Aqueous-phase equilibrium

Equilibrium	K (M)	$\Delta H/R$ (K)	Ref.
$\text{CO}_2 + \text{H}_2\text{O} \rightleftharpoons \text{H}^+ + \text{HCO}_3^-$	4.2×10^{-7}		Cotton and Wilkinson (1967)
$\text{HCO}_3^- \rightleftharpoons \text{H}^+ + \text{CO}_3^{2-}$	4.8×10^{-11}		Cotton and Wilkinson (1967)
$\text{SO}_2 + \text{H}_2\text{O} \rightleftharpoons \text{H}^+ + \text{HSO}_3^-$	1.7×10^{-2}	-2.09×10^3	NBS (1965)
$\text{HSO}_3^- \rightleftharpoons \text{H}^+ + \text{SO}_3^{2-}$	6.3×10^{-8}	-1.51×10^3	NBS (1965)
$\text{HNO}_3 \rightleftharpoons \text{H}^+ + \text{NO}_3^-$	2.2×10^1		NBS (1965)
$\text{HO}_2 \rightleftharpoons \text{H}^+ + \text{O}_2^-$	2.0×10^{-5}		Bielski (1978)
$\text{HCOOH} \rightleftharpoons \text{H}^+ + \text{HCOO}^-$	1.8×10^{-4}	1.50×10^2	Sillen and Martell (1964)
$\text{H}_2\text{O}_2 \rightleftharpoons \text{H}^+ + \text{HO}_2^-$	2.2×10^{-12}	-3.73×10^3	Smith and Martell (1976)
$\text{HNO}_2 \rightleftharpoons \text{H}^+ + \text{NO}_2^-$	5.0×10^{-4}	1.70×10^3	NBS (1965)
$\text{HNO}_4 \rightleftharpoons \text{H}^+ + \text{NO}_4^-$	1.4×10^{-6}		Logager and Sehested (1993)
$\text{CH}_2\text{O} + \text{H}_2\text{O} \rightleftharpoons \text{CH}_2(\text{OH})_2$	2.5×10^{3a}	-4.03×10^3	Bell (1966)
$\text{HCl} \rightleftharpoons \text{H}^+ + \text{Cl}^-$	1.7×10^6	-6.89×10^3	Marsh and McElroy (1985)
$\text{NH}_3 + \text{H}_2\text{O} \rightleftharpoons \text{NH}_4^+ + \text{OH}^-$	1.7×10^{-5}	4.32×10^3	NBS (1965)

^a K without unity.

Table 3
 HO_x chemistry in droplets

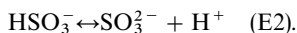
Reactions		$k_{298} (\text{M}^{-n+1} \text{s}^{-1})$	E_a/R (K)	Ref.
$\text{O}_3 + \text{h}\nu + \text{H}_2\text{O} \rightarrow \text{H}_2\text{O}_2 + \text{O}_2$	(A1)	Calculated		Graedel and Weschler (1981)
$\text{H}_2\text{O}_2 + \text{h}\nu \rightarrow 2\text{OH}$	(A2)	Calculated		Graedel and Weschler (1981) and Zellner et al. (1990)
$\text{OH} + \text{HO}_2 \rightarrow \text{H}_2\text{O} + \text{O}_2$	(A3)	2.8×10^{10}	0	Elliot and Buxton (1992)
$\text{OH} + \text{O}_2^- \rightarrow \text{HO}^- + \text{O}_2$	(A4)	3.5×0^{10}	720	Elliot and Buxton (1992)
$\text{H}_2\text{O}_2 + \text{OH} \rightarrow \text{H}_2\text{O} + \text{HO}_2$	(A5)	2.7×10^7	1700	Christensen et al. (1982)
$\text{HO}_2 + \text{HO}_2 \rightarrow \text{H}_2\text{O}_2 + \text{O}_2$	(A6)	8.6×10^5	2700	Bielski (1978)
$\text{HO}_2 + \text{O}_2^- + \text{H}_2\text{O} \rightarrow \text{H}_2\text{O}_2 + \text{O}_2 + \text{OH}^-$	(A7)	1×10^8	910	Christensen and Sehested (1988)
$\text{O}_3 + \text{HO}_2 \rightarrow \text{OH} + 2\text{O}_2$	(A8)	$< 1 \times 10^4$		Sehested et al. (1984)
$\text{O}_3 + \text{O}_2^- + \text{H}_2\text{O} \rightarrow \text{OH} + 2\text{O}_2 + \text{OH}^-$	(A9)	1.5×10^9		Sehested et al. (1983)
$\text{OH} + \text{HSO}_3^- \rightarrow \text{SO}_3^- + \text{H}_2\text{O}$	(A10)	2.7×10^9		Buxton et al. (1996a)
$\text{OH} + \text{SO}_3^{2-} \rightarrow \text{SO}_3^- + \text{OH}^-$	(A11)	4.6×10^9		Buxton et al. (1996a)

CH_3 , OHCH_2) and the production of OHCH_2O_2 radical in the oxidation chain of methanol (A101–A105) which, in their paper, directly leads to the production of formaldehyde and HO_2 radical. But, the OHCH_2O_2 radical can produce significant amount of formic acid by its self-reaction (A86), related to the methanol concentration and pH dependence (Monod and Carlier, 1999; Monod et al., 2000). Moreover, only its decomposition (A82) produces HO_2 radical and formaldehyde. More generally, the development of a tropospheric aqueous mechanism, even excluding transient metals, and $\text{C} > 2$ species, is still subject to many uncertainties in rate constants values (in Tables 3–8, many rate constants are estimated and their temperature dependency is not available).

2.2. Mathematical formulation

The gases that are scavenged by the droplets and that are involved in aqueous-phase equilibrium are listed in

Table 2 and are treated in the model as total species. This treatment prevents from losing mass. As an example, sulfur dioxide dissociates twice:



In the model, the concentrations of the two ions are not explicitly calculated. The concentration predicted for sulfur dioxide in aqueous phase is the total sulfur concentration

$$[\text{SO}_2(\text{w})] = [\text{SO}_2(\text{l})] + [\text{HSO}_3^-] + [\text{SO}_3^{2-}].$$

Thus, rate constants for such total species are derived with including the fraction of the total species considered. As an example, the rate constant of the reaction A3 is derived as follows: $k_{\text{A3}}^m = k_{\text{A3}}^i [\text{H}^+] / K_{\text{HO}_2} + [\text{H}^+]$, where k_{A3}^m is the rate constant calculated in the model, k_{A3}^i is the

Table 4
Chlorine chemistry in droplets

Reactions		$k_{298}(\text{M}^{-n+1} \text{s}^{-1})$	E_a/R (K)	Ref.
$\text{Cl}^- + \text{OH} \rightarrow \text{OHCl}^-$	(A12)	4.3×10^9		Jayson et al. (1973)
$\text{OHCl}^- \rightarrow \text{Cl}^- + \text{OH}$	(A13)	6.1×10^9		Jayson et al. (1973)
$\text{OHCl}^- + \text{H}^+ \rightarrow \text{Cl} + \text{H}_2\text{O}$	(A14)	2.1×10^{10}		Jayson et al. (1973)
$\text{Cl} + \text{H}_2\text{O} \rightarrow \text{OHCl}^- + \text{H}^+$	(A15)	1.3×10^3		Jayson et al. (1973)
$\text{Cl} + \text{Cl}^- \rightarrow \text{Cl}_2^-$	(A16)	2.7×10^{10}		Jacobi et al. (1997)
$\text{Cl}_2^- \rightarrow \text{Cl} + \text{Cl}^-$	(A17)	1.4×10^5		Jacobi et al. (1997)
$\text{Cl}_2^- + \text{Cl}_2^- \rightarrow \text{Cl}_2 + 2\text{Cl}^-$	(A18)	8.7×10^8		Zellner et al. (1996)
$\text{Cl}_2 + \text{H}_2\text{O} \rightarrow \text{H}^+ + \text{Cl}^- + \text{HOCl}$	(A19)	22.3	7600	Wang and Margerum (1994)
$\text{Cl}^- + \text{HOCl} + \text{H}^+ \rightarrow \text{Cl}_2 + \text{H}_2\text{O}$	(A20)	4.4×10^4		Wang and Margerum (1994)
$\text{HOCl} + \text{HO}_2 \rightarrow \text{H}_2\text{O} + \text{O}_2 + \text{Cl}$	(A21)	$7.5 \times 10^6 = k_{22}$		Estimated
$\text{HOCl} + \text{O}_2^- \rightarrow \text{OH}^- + \text{O}_2 + \text{Cl}$	(A22)	7.5×10^6		Long and Bielski (1980)
$\text{Cl}_2 + \text{HO}_2 \rightarrow \text{Cl}_2^- + \text{O}_2 + \text{H}^+$	(A23)	1×10^9		Bjergbakke et al. (1981)
$\text{Cl}_2 + \text{O}_2^- \rightarrow \text{Cl}_2^- + \text{O}_2$	(A24)	$1 \times 10^9 = k_{23}$		Estimated
$\text{Cl} + \text{HO}_2 \rightarrow \text{O}_2 + \text{Cl}^- + \text{H}^+$	(A25)	3.1×10^9	1500	Graedel and Goldberg (1983)
$\text{Cl} + \text{H}_2\text{O}_2 \rightarrow \text{HO}_2 + \text{Cl}^- + \text{H}^+$	(A26)	4.5×10^7		Graedel and Goldberg (1983)
$\text{Cl}^- + \text{NO}_3 \rightarrow \text{NO}_3^- + \text{Cl}$	(A27)	1×10^7	4300	Exner et al. (1992)
$\text{Cl}^- + \text{SO}_4^- \rightarrow \text{SO}_4^{2-} + \text{Cl}$	(A28)	3.3×10^8	0	Herrmann et al. (1997)
$\text{Cl}_2^- + \text{HO}_2 \rightarrow \text{O}_2 + 2\text{Cl}^- + \text{H}^+$	(A29)	1.3×10^{10}		Jacobi (1996)
$\text{Cl}_2^- + \text{O}_2^- \rightarrow \text{O}_2 + 2\text{Cl}^-$	(A30)	6×10^9		Jacobi (1996)
$\text{Cl}_2^- + \text{H}_2\text{O}_2 \rightarrow \text{HO}_2 + 2\text{Cl}^- + \text{H}^+$	(A31)	7×10^5	3300	Elliot (1989)
$\text{Cl}_2^- + \text{OH}^- \rightarrow 2\text{Cl}^- + \text{OH}$	(A32)	4×10^6		Jacobi (1996)
$\text{Cl}_2^- + \text{HSO}_3^- \rightarrow \text{SO}_3^- + 2\text{Cl}^- + \text{H}^+$	(A33)	1.7×10^8	400	Jacobi et al. (1996)
$\text{Cl}_2^- + \text{SO}_3^{2-} \rightarrow \text{SO}_3^- + 2\text{Cl}^-$	(A34)	6.2×10^7		Jacobi et al. (1996)

Table 5
Carbonate chemistry in droplets

Reactions		$k_{298}(\text{M}^{-n+1} \text{s}^{-1})$	E_a/R (K)	Ref.
$\text{HCO}_3^- + \text{OH} \rightarrow \text{H}_2\text{O} + \text{CO}_3^-$	(A35)	1.7×10^7	1900	Herrmann et al. (1999a)
$\text{CO}_3^{2-} + \text{OH} \rightarrow \text{OH}^- + \text{CO}_3^-$	(A36)	1×10^9	2550	Buxton et al. (1988)
$\text{HCO}_3^- + \text{O}_2^- \rightarrow \text{HO}_2^- + \text{CO}_3^-$	(A37)	1.5×10^6		Schmidt (1972)
$\text{CO}_3^{2-} + \text{NO}_3 \rightarrow \text{NO}_3^- + \text{CO}_3^-$	(A38)	4.1×10^7		Estimated from Herrmann et al. (2000)
$\text{CO}_3^{2-} + \text{Cl}_2^- \rightarrow 2\text{Cl}^- + \text{CO}_3^-$	(A39)	2.7×10^6		Estimated from Herrmann et al. (2000)
$\text{HCO}_3^- + \text{SO}_4^- \rightarrow \text{SO}_4^{2-} + \text{H}^+ + \text{CO}_3^-$	(A40)	2.8×10^6	2100	Huie and Clifton (1990)
$\text{CO}_3^{2-} + \text{SO}_4^- \rightarrow \text{SO}_4^{2-} + \text{CO}_3^-$	(A41)	4.1×10^6	3200	Padmaja et al. (1993)
$\text{CO}_3^- + \text{CO}_3^- + \text{O}_2 \rightarrow 2\text{O}_2^- + 2\text{CO}_2$	(A42)	2.2×10^6		Huie and Clifton (1990)
$\text{CO}_3^- + \text{HO}_2 \rightarrow \text{HCO}_3^- + \text{O}_2$	(A43)	$6.5 \times 10^8 = k_{44}$		Estimated
$\text{CO}_3^- + \text{O}_2^- \rightarrow \text{CO}_3^{2-} + \text{O}_2$	(A44)	6.5×10^8		Eriksen et al. (1985)
$\text{CO}_3^- + \text{H}_2\text{O}_2 \rightarrow \text{HO}_2 + \text{HCO}_3^-$	(A45)	4.3×10^5		Draganic et al. (1991)
$\text{CO}_3^- + \text{HSO}_3^- \rightarrow \text{HCO}_3^- + \text{SO}_3^-$	(A46)	1×10^7		Estimated from Herrmann et al. (2000)
$\text{CO}_3^- + \text{SO}_3^{2-} \rightarrow \text{CO}_3^{2-} + \text{SO}_3^-$	(A47)	2.9×10^7	470	Huie et al. (1991)

real rate constant listed in Table 3 and K_{HO_2} is the dissociation constant of HO_2 radical listed in Table 2.

The mathematical formulation of the set of differential equations is written as

$$\frac{dC_g^i}{dt} = P_g^i - D_g^i C_g^i + \frac{k_t C_w^i}{H^* RT} - L k_t C_g^i, \quad (1)$$

$$\frac{dC_w^i}{dt} = P_w^i - D_w^i C_w^i + L k_t C_g^i - \frac{k_t C_w^i}{H^* RT}, \quad (2)$$

where C_g^i and C_w^i are, respectively, the gaseous and aqueous concentrations of the species i in molec cm^{-3} ; P_g^i and P_w^i , and D_g^i and D_w^i are respectively the gaseous and aqueous production terms of the species i in $\text{molec cm}^{-3} \text{s}^{-1}$; and the gaseous and aqueous destruction terms of the species i in s^{-1} , k_t describes the mass transfer between gas and aqueous phases of the species i , L is the liquid water content in vol/vol , H^* is the Henry law effective constant of the species i in M atm^{-1} and $R = 0.08206 \text{ atm M}^{-1} \text{ K}^{-1}$. The transfer rate constant

Table 6
N-chemistry in droplets

Reactions		$k_{298}(\text{M}^{-n+1} \text{s}^{-1})$	E_a/R (K)	Ref.
$\text{HNO}_2 + \text{h}\nu \rightarrow \text{NO} + \text{OH}$	(A48)	Calculated		Graedel and Weschler (1981)
$\text{NO}_2^- + \text{h}\nu + \text{H}_2\text{O} \rightarrow \text{NO} + \text{OH} + \text{OH}^-$	(A49)	Calculated		Graedel and Weschler (1981) and Zellner et al. (1990)
$\text{HNO}_2 + \text{OH} \rightarrow \text{NO}_2 + \text{H}_2\text{O}$	(A50)	1×10^9		Rettich (1978)
$\text{NO}_2^- + \text{OH} \rightarrow \text{NO}_2 + \text{OH}^-$	(A51)	1×10^{10}		Treinin (1970)
$\text{HNO}_2 + \text{H}_2\text{O}_2 + \text{H}^+ \rightarrow \text{NO}_3^- + 2\text{H}^+ + \text{H}_2\text{O}$	(A52)	6.3×10^3	6700	Lee and Lind (1986)
$\text{NO}_2^- + \text{O}_3 \rightarrow \text{NO}_3^- + \text{O}_2$	(A53)	5×10^5	6900	Damschen and Martin (1983)
$\text{NO}_2^- + \text{NO}_3 \rightarrow \text{NO}_2 + \text{NO}_3^-$	(A54)	1.2×10^9		Daniels (1968)
$\text{NO}_2^- + \text{Cl}_2 \rightarrow \text{NO}_2 + 2\text{Cl}^-$	(A55)	6×10^7		Herrmann et al. (1999a)
$\text{NO}_2^- + \text{CO}_3^- \rightarrow \text{NO}_2 + \text{CO}_3^{2-}$	(A56)	6.6×10^5	850	Huie et al. (1991)
$\text{NO}_2 + \text{OH} \rightarrow \text{NO}_3^- + \text{H}^+$	(A57)	1.2×10^{10}		Wagner et al. (1980)
$\text{NO}_2 + \text{HO}_2 \rightarrow \text{HNO}_4$	(A58)	1.8×10^9		Logager and Sehested (1993)
$\text{NO}_2 + \text{O}_2^- \rightarrow \text{NO}_4^-$	(A59)	4.5×10^9		Logager and Sehested (1993)
$\text{HNO}_4 \rightarrow \text{HO}_2 + \text{NO}_2$	(A60)	4.6×10^{-3}		Lammel et al. (1990)
$\text{HNO}_4 \rightarrow \text{HNO}_2 + \text{O}_2$	(A61)	7×10^{-4}		Logager and Sehested (1993)
$\text{NO}_4^- \rightarrow \text{NO}_2^- + \text{O}_2$	(A62)	1		Logager and Sehested (1993)
$\text{HNO}_4 + \text{HSO}_3^- \rightarrow \text{SO}_4^{2-} + \text{NO}_3^- + 2\text{H}^+$	(A63)	3.3×10^5		Amels et al. (1966)
$\text{NO}_2 + \text{NO}_2 + \text{H}_2\text{O} \rightarrow \text{HNO}_2 + \text{NO}_3^- + \text{H}^+$	(A64)	8.4×10^7	- 2900	Park and Lee (1988)
$\text{NO}_2 + \text{NO} + \text{H}_2\text{O} \rightarrow 2\text{NO}_2^- + 2\text{H}^+$	(A65)	3×10^8		Hoffmann and Calvert (1985)
$\text{NO} + \text{OH} \rightarrow \text{NO}_2^- + \text{H}^+$	(A66)	2×10^{10}	1500	Strehlow and Wagner (1982)
$\text{NO}_3^- + \text{h}\nu + \text{H}_2\text{O} \rightarrow \text{NO}_2 + \text{OH} + \text{OH}^-$	(A67)	Calculated		Graedel and Weschler (1981) and Zellner et al. (1990)
$\text{N}_2\text{O}_5 + \text{H}_2\text{O} \rightarrow 2\text{HNO}_3$	(A68)	1×10^{15}		Estimated
$\text{NO}_3 + \text{h}\nu \rightarrow \text{NO} + \text{O}_2$	(A69)	Calculated		Graedel and Weschler (1981)
$\text{NO}_3 + \text{HO}_2 \rightarrow \text{NO}_3^- + \text{H}^+ + \text{O}_2$	(A70)	3×10^9		Sehested et al. (1994)
$\text{NO}_3 + \text{O}_2^- \rightarrow \text{NO}_3^- + \text{O}_2$	(A71)	$3 \times 10^9 = k_{70}$		Estimated
$\text{NO}_3 + \text{H}_2\text{O}_2 \rightarrow \text{NO}_3^- + \text{H}^+ + \text{HO}_2$	(A72)	4.9×10^6	2000	Herrmann et al. (1994)
$\text{NO}_3 + \text{OH}^- \rightarrow \text{NO}_3^- + \text{OH}$	(A73)	9.4×10^7	2700	Exner et al. (1992)
$\text{NO}_3 + \text{HSO}_4^- \rightarrow \text{NO}_3^- + \text{H}^+ + \text{SO}_4^-$	(A74)	5.6×10^3		Herrmann et al. (1999a)
$\text{NO}_3 + \text{SO}_4^{2-} \rightarrow \text{NO}_3^- + \text{SO}_4^-$	(A75)	1×10^5		Logager et al. (1993)
$\text{NO}_3 + \text{HSO}_3^- \rightarrow \text{SO}_3^- + \text{NO}_3^- + \text{H}^+$	(A76)	1.3×10^9	2200	Exner et al. (1992)
$\text{NO}_3 + \text{SO}_3^{2-} \rightarrow \text{NO}_3^- + \text{SO}_3^-$	(A77)	3×10^8		Exner et al. (1992)

k_i is the inverse of characteristic times for gaseous diffusion and for interfacial mass transport (Schwartz, 1986):

$$k_i = \left(\frac{a^2}{3D_g} + \frac{4a}{3\bar{v}\alpha} \right)^{-1}, \quad (3)$$

where a is the droplet radius in cm, D_g is the gaseous diffusion coefficient taken equal to $0.1 \text{ cm}^2 \text{ s}^{-1}$ for all species, $\bar{v} = \sqrt{8\bar{R}T/\pi M^i}$ is the mean quadratic speed of the species i in cm s^{-1} (M^i is the molar mass of the species i and $\bar{R} = 8.3145 \times 10^7 \text{ g cm}^2 \text{ s}^{-2} \text{ K}^{-1} \text{ mol}^{-1}$) and α is the accommodation of the species i listed in Table 1.

The pH of the droplets is calculated at each time step by solving a simplified ionic balance equation written as.

$$\begin{aligned} [\text{H}^+] + [\text{NH}_4^+] &= [\text{OH}^-] + [\text{HCO}_3^-] + [\text{NO}_3^-] \\ &+ [\text{HSO}_3^-] + [\text{Cl}^-] + \sum v_i[\text{ions}], \end{aligned} \quad (4)$$

where $\sum [\text{ions}]$ is the sum of ions produced in the droplets and v_i is the number of charges carried by the considered ion. Each ionic concentration is expressed as a function of the total concentration of the gaseous species scavenged by droplets. The pH is calculated after solving a polynomial of degree 8. This resolution is made by a variant of Laguerre's method (Wilkinson, 1965; Smith, 1967). This method is more computing time efficient.

2.3. Partitioning of species between phases

Following the kinetic formulation of mass transfer defined in Schwartz (1986), the tropospheric trace species in presence of clouds do not all follow the Henry's law equilibrium. In order to evaluate if the species diverges from Henry's law equilibrium, we used a partitioning q factor which expresses the deviation from Henry's law

Table 7
Organic chemistry in droplets

Reactions		$k_{298}(M^{-n+1} s^{-1})$	E_a/R (K)	Ref.
$CH_3O_2 + HO_2 \rightarrow CH_3OOH + O_2$	(A78)	$4.3 \times 10^5 = k_6/2$	3000	Estimated like Jacob (1986)
$CH_3O_2 + O_2^- + H_2O \rightarrow CH_3OOH + O_2 + OH^-$	(A79)	$5 \times 10^7 = k_7/2$	1600	Estimated like Jacob (1986)
$CH_3O_2 + CH_3O_2 \rightarrow CH_3OH + CH_2O + O_2$	(A80)	1.7×10^8	2200	Herrmann et al. (1999b)
$CH_3O_2 + HSO_3^- \rightarrow CH_3OOH + SO_3^-$	(A81)	5×10^5		Herrmann et al. (1999b)
$OHCH_2O_2 + H_2O \rightarrow H_2C(OH)_2 + HO_2$	(A82)	6	7000	Estimated from Monod and Carlier (1999)
$OHCH_2O_2 + OH^- + H_2O \rightarrow H_2C(OH)_2 + HO_2 + OH^-$	(A83)	2.1×10^{10}	7200	Monod and Carlier (1999)
$OHCH_2O_2 + HO_2 \rightarrow OHCH_2OOH + O_2$	(A84)	$4.3 \times 10^5 = k_{78}$	3000	Estimated
$OHCH_2O_2 + O_2^- + H_2O \rightarrow OHCH_2OOH + O_2 + OH^-$	(A85)	$5 \times 10^7 = k_{79}$	1600	Estimated
$OHCH_2O_2 + OHCH_2O_2 \rightarrow 2HCOOH + H_2O_2$	(A86)	7.4×10^8	1400	Huie and Clifton (1993)
$OHCH_2OOH + hv + O_2 \rightarrow HCOOH + OH + HO_2$	(A87)	Estimated = $J(H_2O_2)$		Graedel and Weschler (1981)
$OHCH_2OOH + OH \rightarrow OHCH_2O_2 + H_2O$	(A88)	$2.7 \times 10^7 = k_5$	1700	Estimated
$OHCH_2OOH + OH \rightarrow HCOOH + OH + H_2O$	(A89)	1.9×10^7 ^(a)	1900	Estimated
$OHCH_2OOH + NO_3 \rightarrow NO_3^- + H^+ + OHCH_2O_2$	(A90)	$4.9 \times 10^6 = k_{72}$	2000	Estimated
$OHCH_2OOH + CO_3^- \rightarrow OHCH_2O_2 + HCO_3^-$	(A91)	$4.3 \times 10^5 = k_{45}$		Estimated
$OHCH_2OOH + Cl_2^- \rightarrow OHCH_2O_2 + 2Cl^- + H^+$	(A92)	$7 \times 10^5 = k_{31}$	3300	Estimated
$OHCH_2OOH + SO_4^- \rightarrow SO_4^{2-} + H^+ + OHCH_2O_2$	(A93)	$2.8 \times 10^7 = k_{147}$		Estimated
$CH_3OOH + hv + O_2 \rightarrow CH_2O + OH + HO_2$	(A94)	Estimated = $J(H_2O_2)$		Graedel and Weschler (1981)
$CH_3OOH + OH \rightarrow CH_3O_2 + H_2O$	(A95)	$2.7 \times 10^7 = k_5$	1700	Estimated like Jacob (1986)
$CH_3OOH + OH \rightarrow CH_2O + OH + H_2O$	(A96)	1.9×10^7 ^(a)	1900	Estimated like Jacob (1986)
$CH_3OOH + NO_3 \rightarrow NO_3^- + H^+ + CH_3O_2$	(A97)	$4.9 \times 10^6 = k_{72}$	2000	Estimated
$CH_3OOH + CO_3^- \rightarrow CH_3O_2 + HCO_3^-$	(A98)	$4.3 \times 10^5 = k_{45}$		Estimated
$CH_3OOH + Cl_2^- \rightarrow CH_3O_2 + 2Cl^- + H^+$	(A99)	$7 \times 10^5 = k_{31}$	3300	Estimated
$CH_3OOH + SO_4^- \rightarrow SO_4^{2-} + H^+ + CH_3O_2$	(A100)	$2.8 \times 10^7 = k_{147}$		Estimated
$CH_3OH + OH + O_2 \rightarrow OHCH_2O_2 + H_2O$	(A101)	1×10^9	600	Elliot and McCracken (1989)
$CH_3OH + NO_3 + O_2 \rightarrow NO_3^- + H^+ + OHCH_2O_2$	(A102)	5.4×10^5	4300	Herrmann et al. (1999a)
$CH_3OH + CO_3^- + O_2 \rightarrow HCO_3^- + OHCH_2O_2$	(A103)	5.7×10^3	3100	Clifton and Huie (1993)
$CH_3OH + Cl_2^- + O_2 \rightarrow 2Cl^- + H^+ + OHCH_2O_2$	(A104)	5×10^4	5500	Jacobi et al. (1999)
$CH_3OH + SO_4^- + O_2 \rightarrow SO_4^{2-} + H^+ + OHCH_2O_2$	(A105)	9×10^6	2200	Clifton and Huie (1989)
$H_2C(OH)_2 + OH + O_2 \rightarrow HCOOH + HO_2 + H_2O$	(A106)	7.8×10^8	1000	Chin and Wine (1994)
$H_2C(OH)_2 + NO_3 + O_2 \rightarrow NO_3^- + H^+ + HO_2 + HCOOH$	(A107)	1×10^6	4500	Exner et al. (1993)
$H_2C(OH)_2 + CO_3^- + O_2 \rightarrow HCO_3^- + HO_2 + HCOOH$	(A108)	1.3×10^4		Zellner et al. (1996)
$H_2C(OH)_2 + Cl_2^- + O_2 \rightarrow 2Cl^- + H^+ + HCOOH + HO_2$	(A109)	3.1×10^4	4400	Jacobi et al. (1999)
$H_2C(OH)_2 + SO_4^- + O_2 \rightarrow SO_4^{2-} + HCOOH + HO_2 + H^+$	(A110)	1.4×10^7	1300	Buxton et al. (1990)
$HCOOH + OH + O_2 \rightarrow CO_2 + HO_2 + H_2O$	(A111)	1×10^8	1000	Chin and Wine (1994)
$HCOO^- + OH + O_2 \rightarrow CO_2 + HO_2 + OH^-$	(A112)	3.4×10^9	1200	Chin and Wine (1994)
$HCOOH + NO_3 + O_2 \rightarrow NO_3^- + H^+ + CO_2 + HO_2$	(A113)	3.8×10^5	3400	Exner et al. (1994)
$HCOO^- + NO_3 + O_2 \rightarrow NO_3^- + CO_2 + HO_2$	(A114)	5.1×10^7	2200	Exner et al. (1994)
$HCOO^- + CO_3^- + H_2O + O_2 \rightarrow CO_2 + HCO_3^- + HO_2 + OH^-$	(A115)	1.4×10^5	3300	Zellner et al. (1996)
$HCOOH + Cl_2^- + O_2 \rightarrow CO_2 + 2Cl^- + HO_2 + H^+$	(A116)	5.5×10^3	4500	Jacobi et al. (1999)
$HCOO^- + Cl_2^- + O_2 \rightarrow CO_2 + 2Cl^- + HO_2$	(A117)	1.3×10^6		Jacobi et al. (1996)
$HCOOH + SO_4^- + O_2 \rightarrow SO_4^{2-} + H^+ + CO_2 + HO_2$	(A118)	2.5×10^6		Herrmann et al. (1999a)
$HCOO^- + SO_4^- + O_2 \rightarrow SO_4^{2-} + CO_2 + HO_2$	(A119)	2.1×10^7		Herrmann et al. (1999a)

^aEstimated from A88 and the branching ratio of the gas phase reaction $CH_3OOH + OH$.

equilibrium for the species i :

$$q = \frac{C_w^i}{LH^*RTC_g^i} \quad (5)$$

This factor is equal to 1 when the species is at Henry's law equilibrium, is less than 1 when the aqueous concentrations of the species do not reach the aqueous Henry's law equilibrium concentration and is greater than 1 when the aqueous concentration of the species is above the equilibrium concentration. The reasons for this deviation from Henry's law equilibrium can be explained by the kinetic of mass transfer limitation for very soluble species or for

high reactivity of species in gaseous and/or aqueous phase (see Chaumerliac et al., 2000; Audiffren et al., 1998 for a detailed discussion on the significance of the q factor).

3. Model results

The multiphase box model is initialized with multiphase measurements made during the European CIME experiment by Voisin et al. (2000) during one cloud event. As a first-step study, we used this experiment to evaluate the main reaction pathways in aqueous phase that we

Table 8
S-chemistry in droplets

Reactions		$k_{298}(\text{M}^{-n+1} \text{s}^{-1})$	E_a/R (K)	Ref.
$\text{HSO}_3^- + \text{CH}_2\text{O} \rightarrow \text{HOCH}_2\text{SO}_3^-$	(A120)	7.9×10^2	2900	Olson and Hoffmann (1989)
$\text{SO}_3^{2-} + \text{CH}_2\text{O} \rightarrow \text{HOCH}_2\text{SO}_3^- + \text{OH}^-$	(A121)	2.5×10^7	- 2450	Olson and Hoffmann (1989)
$\text{HOCH}_2\text{SO}_3^- \rightarrow \text{HSO}_3^- + \text{CH}_2\text{O}$	(A122)	7.7×10^{-3}	9200	Möller and Mauersberger (1995)
$\text{HOCH}_2\text{SO}_3^- + \text{OH}^- \rightarrow \text{SO}_3^{2-} + \text{CH}_2(\text{OH})_2$	(A123)	3.7×10^3		Deister et al. (1986)
$\text{HOCH}_2\text{SO}_3^- + \text{OH} + \text{O}_2 \rightarrow \text{HO}_2 + \text{HCOOH} + \text{HSO}_3^-$	(A124)	3×10^8		Buxton (1994)
$\text{HOCH}_2\text{SO}_3^- + \text{NO}_3 \rightarrow \text{NO}_3^- + \text{H}^+ + \text{CH}_2\text{O} + \text{SO}_3^-$	(A125)	4.2×10^6		Herrmann et al. (1999a)
$\text{HOCH}_2\text{SO}_3^- + \text{Cl}_2^- \rightarrow 2\text{Cl}^- + \text{H}^+ + \text{CH}_2\text{O} + \text{SO}_3^-$	(A126)	5×10^5		Jacobi et al. (1996)
$\text{HOCH}_2\text{SO}_3^- + \text{SO}_4^- \rightarrow \text{SO}_4^{2-} + \text{H}^+ + \text{CH}_2\text{O} + \text{SO}_3^-$	(A127)	2.8×10^6		Buxton (1994)
$\text{SO}_5^- + \text{O}_2 \rightarrow \text{SO}_5^-$	(A128)	2.5×10^9		Buxton et al. (1996b)
$\text{SO}_5^- + \text{HSO}_3^- \rightarrow \text{HSO}_5^- + \text{SO}_3^-$	(A129)	8.6×10^3		Buxton et al. (1996b)
$\text{SO}_5^- + \text{HSO}_3^- \rightarrow \text{SO}_4^- + \text{SO}_4^{2-} + \text{H}^+$	(A130)	3.6×10^2		Buxton et al. (1996b)
$\text{SO}_5^- + \text{SO}_3^{2-} \rightarrow \text{HSO}_5^- + \text{SO}_3^- + \text{OH}^-$	(A131)	2.1×10^5		Buxton et al. (1996b)
$\text{SO}_5^- + \text{SO}_3^{2-} \rightarrow \text{SO}_4^- + \text{SO}_4^{2-}$	(A132)	5.5×10^5		Buxton et al. (1996b)
$\text{SO}_5^- + \text{HO}_2 \rightarrow \text{HSO}_5^- + \text{O}_2$	(A133)	1.7×10^9		Buxton et al. (1996a)
$\text{SO}_5^- + \text{O}_2^- + \text{H}_2\text{O} \rightarrow \text{HSO}_5^- + \text{O}_2 + \text{OH}^-$	(A134)	$1.7 \times 10^9 = k_{133}$		Estimated
$\text{SO}_5^- + \text{SO}_5^- \rightarrow 2\text{SO}_4^- + \text{O}_2$	(A135)	7.2×10^6	2600	Herrmann et al. (1995)
$\text{SO}_5^- + \text{SO}_5^- \rightarrow \text{S}_2\text{O}_8^{2-} + \text{O}_2$	(A136)	1.8×10^8	2600	Herrmann et al. (1995)
$\text{HSO}_5^- + \text{HSO}_3^- + \text{H}^+ \rightarrow 2\text{SO}_4^{2-} + 3\text{H}^+$	(A137)	7.1×10^6		Betterton and Hoffmann (1988b)
$\text{HSO}_5^- + \text{SO}_3^{2-} + \text{H}^+ \rightarrow 2\text{SO}_4^{2-} + 2\text{H}^+$	(A138)	$7.1 \times 10^6 = k_{137}$		Estimated
$\text{HSO}_5^- + \text{OH}^- \rightarrow \text{SO}_5^- + \text{H}_2\text{O}$	(A139)	1.7×10^7	1900	Maruthamuthu and Neta (1977)
$\text{SO}_4^- + \text{SO}_4^- \rightarrow \text{S}_2\text{O}_8^{2-}$	(A140)	4.4×10^8	0	Huie and Clifton (1993)
$\text{SO}_4^- + \text{H}_2\text{O} \rightarrow \text{SO}_4^{2-} + \text{OH} + \text{H}^+$	(A141)	11	1100	Herrmann et al. (1995)
$\text{SO}_4^- + \text{HSO}_3^- \rightarrow \text{SO}_4^{2-} + \text{H}^+ + \text{SO}_3^-$	(A142)	3.2×10^8		Herrmann et al. (1999a)
$\text{SO}_4^- + \text{SO}_3^- \rightarrow \text{SO}_4^{2-} + \text{SO}_3^-$	(A143)	3.2×10^8	1200	Herrmann et al. (1999a)
$\text{SO}_4^- + \text{HO}_2 \rightarrow \text{SO}_4^{2-} + \text{H}^+ + \text{O}_2$	(A144)	3.5×10^9		Jiang et al. (1992)
$\text{SO}_4^- + \text{O}_2^- \rightarrow \text{SO}_4^{2-} + \text{O}_2$	(A145)	$3.5 \times 10^9 = k_{144}$		Estimated
$\text{SO}_4^- + \text{OH}^- \rightarrow \text{SO}_4^{2-} + \text{OH}$	(A146)	1.4×10^7		Herrmann et al. (1995)
$\text{SO}_4^- + \text{H}_2\text{O}_2 \rightarrow \text{SO}_4^{2-} + \text{HO}_2 + \text{H}^+$	(A147)	2.8×10^7		Herrmann et al. (1999a)
$\text{SO}_4^- + \text{NO}_3^- \rightarrow \text{SO}_4^{2-} + \text{NO}_3$	(A148)	5×10^4		Exner et al. (1992)
$\text{SO}_4^- + \text{NO}_2^- \rightarrow \text{SO}_4^{2-} + \text{NO}_2$	(A149)	9.8×10^8		Wine et al. (1989)
$\text{HSO}_4^- + \text{OH}^- \rightarrow \text{H}_2\text{O} + \text{SO}_4^-$	(A150)	3.5×10^5		Tang et al. (1988)
$\text{HSO}_4^- \rightarrow \text{SO}_4^{2-} + \text{H}^+$	(A151)	1×10^9	- 2700	Redlich (1946)
$\text{SO}_4^{2-} + \text{H}^+ \rightarrow \text{HSO}_4^-$	(A152)	1×10^{11}		Graedel and Weschler (1981)
$\text{HSO}_3^- + \text{O}_3 \rightarrow \text{HSO}_4^- + \text{O}_2$	(A153)	3.7×10^5	5500	Hoffmann (1986)
$\text{SO}_3^{2-} + \text{O}_3 \rightarrow \text{SO}_4^{2-} + \text{O}_2$	(A154)	1.5×10^9	5300	Hoffmann (1986)
$\text{HSO}_3^- + \text{H}_2\text{O}_2 + \text{H}^+ \rightarrow \text{SO}_4^{2-} + 2\text{H}^+ + \text{H}_2\text{O}$	(A155)	9.1×10^7	3600	Maaß et al. (1999)
$\text{HSO}_3^- + \text{CH}_3\text{OOH} + \text{H}^+ \rightarrow \text{SO}_4^{2-} + 2\text{H}^+ + \text{CH}_3\text{OH}$	(A156)	1.8×10^7	3800	Lind et al. (1987)

considered in our chemical model and to attempt some qualitative comparisons with real environmental data. In parallel, we use these real data to discuss possible discrepancies with more theoretical work as in Herrmann et al. (2000).

3.1. Description of the experiment

The measurements were made during the CIME experiment. This experiment took place at the top of the Puy de Dôme (1465 m), a station located in the center of France during winter 1997 and winter 1998. This station continuously measures temperature, intensity and horizontal wind direction, ozone concentration, sulfur dioxide and NO_x . The station is equipped with a wind tunnel that allows measurements of liquid water content, ice water content and effective radius. The multiphase measurements were performed by Voisin et al. (2000) in

the presence of mixed-phase clouds and liquid clouds (composed of supercooled droplets) and took place from December the 2nd to December the 5th and from December the 12th to December the 13th 1997. The selected day for the simulation is December 13th as on that particular day, there was no ice and the meteorological situation was greatly stable with the presence of strato-cumulus made of supercooled droplets without rain.

The 13th December, the Puy de Dôme was located in an area of transition between a low-pressure system over Eastern Europe and an anticyclone over England at 12 a.m. GMT. Fig. 1a shows the intensity and direction of the horizontal wind at 12 a.m. GMT and at 850 hPa (corresponding to the altitude of the mountain top) and the back-trajectory from the summit computed at 12 a.m. GMT from the CEPMMT model data. The Puy de Dôme mountain is located in a remote environment but on this day, Fig. 1a shows a very strong synoptic

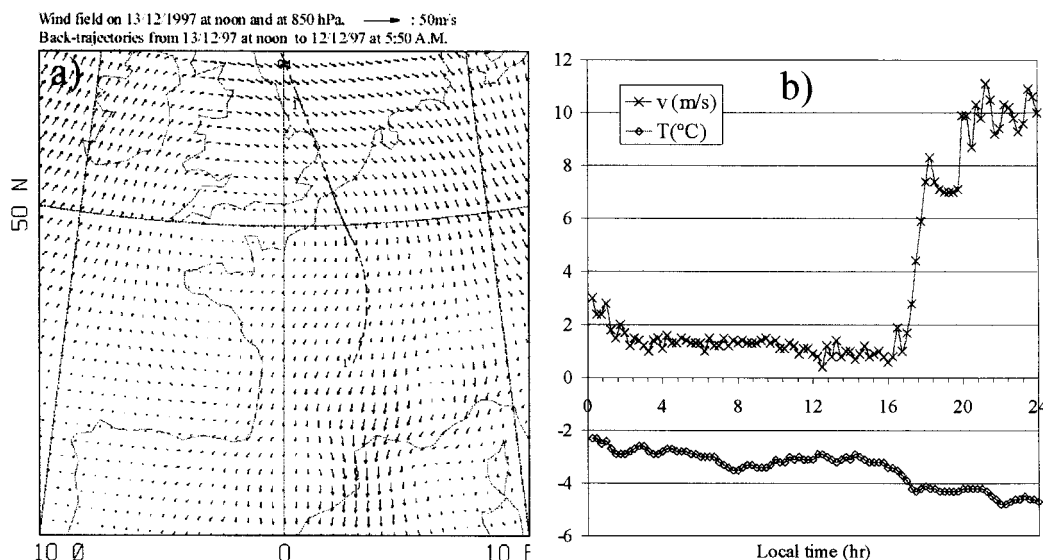


Fig. 1. Meteorological situation at the top at the Puy de Dôme on the 13th December 1997. (a) Horizontal wind intensity and direction at 12 a.m. GMT computed by the CEPMMT model, the solid line corresponds to the back-trajectory from the top of the Puy de Dôme at 12 a.m. GMT. (b) Observed temperature and horizontal wind intensity versus local time.

Table 9

Chemical measurements performed by Voisin et al. (2000) the 13th of December between 10.47 a.m. local time and 3 p.m. local time and mean values liquid water content

Gaseous phase (ppbv^a)

Period of sampling	HCOOH	HCl	HNO ₂	HNO ₃	NH ₃	SO ₂
10.47 a.m.–12.15 a.m.	0.2846	0.0739	0.0540	0.1526	0.1340	0.4484
12.34 a.m.–2.12 p.m.	0.2070	0.1250	0.0369	0.4426	0.1265	0.4891
2.31 p.m.–3.26 p.m.	0.2350	0.1319	0.0470	0.4389	0.0725	0.6371

Aqueous phase (M)

Period of sampling	HCOOH total	Cl ⁻	Nitrite total	Nitrate total	Ammonia total	S(IV) total ^s	Sulfate	pH	LWC (g m ⁻³)
10.47 a.m.–11.30 a.m.	6.19×10^{-6}	1.78×10^{-4}	3.05×10^{-6}	6.96×10^{-4}	2.93×10^{-4}	8.36×10^{-7}	1.60×10^{-4}	3.2	0.151
11.30 a.m.–12.15 a.m.	3.66×10^{-6}	1.04×10^{-4}	2.15×10^{-6}	4.00×10^{-4}	1.67×10^{-4}	3.81×10^{-7}	9.51×10^{-5}	3.4	0.268
12.34 a.m.–1.15 p.m.	6.19×10^{-6}	1.60×10^{-4}	3.32×10^{-6}	6.94×10^{-4}	2.81×10^{-4}	6.56×10^{-7}	1.35×10^{-4}	3.3	0.157
1.15 p.m.–1.30 p.m.	6.02×10^{-6}	1.19×10^{-4}	2.98×10^{-6}	5.37×10^{-4}	2.48×10^{-4}	5.21×10^{-7}	1.00×10^{-4}	3.4	0.220
1.30 p.m.–2.00 p.m.	1.16×10^{-5}	2.69×10^{-4}	5.71×10^{-6}	1.16×10^{-3}	4.47×10^{-4}	1.09×10^{-6}	2.40×10^{-4}	3.1	0.124
2.00 p.m.–2.26 p.m.	1.5×10^{-5}	2.38×10^{-4}	5.59×10^{-6}	1.16×10^{-3}	5.01×10^{-4}	1.00×10^{-6}	1.95×10^{-4}	3.2	0.127
2.31 p.m.–3.00 p.m.	1.64×10^{-5}	3.33×10^{-4}	6.17×10^{-6}	1.98×10^{-3}	6.89×10^{-4}	1.65×10^{-6}	2.43×10^{-4}	3.1	0.091

^a1 ppbv = 2.31×10^{10} molec cm³ of air at $T = 270$ K and $P = 850$ hPa; ^sS(IV) total = [SO₂] + [HSO₃⁻] + [SO₃²⁻] + [HMSA].

influence inducing a polluted air mass coming from the North–NorthEast. Fig. 1b indicates the temperature and the intensity of the wind observed at this day at the station. This figure illustrates a negative temperature all along the day and a low intensity of the wind before 4 p.m. local time. The data obtained for the liquid water content show two cloud events on that day with a transition around 4 p.m. local time. Since Fig. 1b shows

an increase in the intensity of the wind after 4 p.m. local time, we retained for the model simulation the first cloudy event which took place in the most stable meteorological situation.

Table 9 summarizes the multiphase measurements made by Voisin et al. (2000) at the 13th of December between 10.47 a.m. and 3.26 p.m. local time. The total aqueous concentrations take into account both dissolved

Table 10
Conditions of the simulation

Duration	T (°K)	P (hPa)	Radius (μm)
12.15 a.m.–3.00 p.m.	270	850	10

and dissociated forms of the considered species. The supercooled droplets were sampled with an impactor by rime collection with a sampling time around 15 to 30 min. Gases were sampled by two mist chambers in series with a minimum sampling time of 30 min and by three denuder tubes mounted in series for HCOOH, NH_3 , HNO_3 and HCl with a minimum sampling time of 2 h. Denuder tubes were used for controlling most of the measurements made with the mist chambers, except SO_2 and HNO_2 . Moreover, HNO_2 is probably oxidized by ozone in HNO_3 in the mist chamber originating an overestimation of gaseous HNO_3 and an underestimation of gaseous HNO_2 . S(IV) concentrations are overestimated because HMSA is completely converted in S(IV) due to some experimental biases. The chemical analysis of all samples are performed by ionic chromatography. The error on gaseous concentrations is around 13–37% and 10–30% on droplets concentrations. The error on pH value is of 0.1 unit of pH. During this event, the pH value was relatively constant with a maximum variation of 0.3. Its value is between 3.1 and 3.4: the very acid cloud water is partly due to high concentrations of sulfate and nitrate. The last value of the liquid water content of 0.09 g m^{-3} (Table 9) seems to indicate cloud evaporation at the end of the event.

3.2. Conditions of the simulation

Table 10 presents the initial conditions of the simulation which starts at 12.15 a.m. and ends at 3 p.m. local time. During this time, the actinic flux does not vary very much and the photolysis coefficients are taken constant and equal to the values at noon. The actinic flux in the interstitial phase is assumed to be equal to the actinic flux in the cloud-free troposphere (Madronitch, 1987) and the actinic flux inside the droplets is taken as twice the actinic flux in the interstitial phase (Ruggaber et al., 1997). The photolysis coefficients in aqueous phase are calculated from the data of Graedel and Weschler (1981) and Zellner et al. (1990). Fig. 1b exhibits no temperature change during this period and, thus, the temperature is taken constant equal to -3°C . The pressure of 850 hPa corresponds to the altitude of top of the Puy de Dôme. The droplet radius is taken constant since no measurements are available. The value of $10 \mu\text{m}$ corresponds to a typical value of the droplet radius for a strato-cumulus cloud (Pruppacher and Klett, 1997). The liquid water

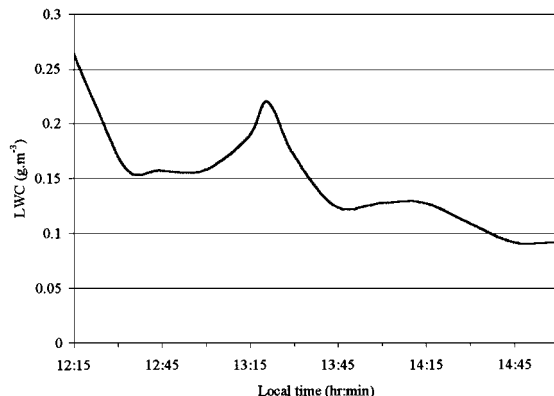


Fig. 2. Time evolution of the liquid water content during simulation.

Table 11
Initial chemical conditions of the simulation

Species	Gaseous concentration (ppbv)	Aqueous concentration (M)
N_2	7.8×10^8	0
O_2	2.1×10^8	0
H_2O	5.7×10^7	cf. LWC
O_3	37	0
NO	0.9	0
NO_2	6.2	0
CH_4	1600	0
CO	100	0
HNO_3	0.15	5.45×10^{-4}
HNO_2	0.054	2.59×10^{-6}
H_2O_2	0.07	0
HCHO	6	0
CH_3OH	2.25	0
SO_2	0.45	6.03×10^{-7a}
HCOOH	0.28	4.89×10^{-6}
NH_3	0.13	2.28×10^{-4}
HCl	0.07	1.40×10^{-4}
S(VI)	0	1.27×10^{-4}

^aCorresponding to total S(IV) = $[\text{SO}_2] + [\text{HSO}_3^-] + [\text{SO}_3^{2-}] + [\text{HMSA}]$.

content is variable and follows the measurements (Table 9), Fig. 2 shows its time evolution during simulation.

Initial chemical conditions are presented in Table 11 for both gas and aqueous phase in the simulation. Initial gas concentrations of NO_x and ozone are deduced from continuous measurements made at the Puy de Dôme station. The other initial gas concentrations correspond to measurements between 10.47 and 12.15 a.m. local time (Table 9). Initial aqueous concentrations are means of measurements performed between 10.47 and 11.30 a.m. local time and between 11.30 and 12.15 a.m. local time

(Table 9). For methane and carbon monoxide, the values are taken from Sillman et al. (1990). For methanol, value is taken from measurements of Leibrock and Slemr (1997) made at an altitude of 1778 m in summer near Garmisch-Partenkirchen in Germany. For hydrogen peroxide, its value is deduced from Noone et al. (1991), who performed measurements in Sweden at a mid-altitude site in strato-cumulus. The initial concentration for formaldehyde is taken from the measurements made during the CIME campaign (P. Laj, personal communication, 1999) on 15th of February 1997 in a polluted air mass with northern origin and in the presence of strato-cumulus without ice (Jeremy et al., 2000).

3.3. Liquid water content sensitivity for measured and simulated aqueous-phase concentrations

As we already explain in the introduction, a strict comparison between observed and model results is difficult to achieve due to the integrated feature of the measurements and to some limitations in the box chemical model. So, order of magnitude and tendencies in the behavior of aqueous-phase species will only be discussed as a function of the varying liquid water content. The set of diagrams in Fig. 3 shows the observed and calculated variations of the pH and of several aqueous-phase concentrations as a function of the liquid water content. Modeling results fairly agree with the data except for low values of the liquid water content (less than 0.1 gm^{-3}) and for formic acid. When the liquid water content is small, the cloud is in fact in its evaporation stage and the cloud droplet radius should decrease so that the aqueous phase should be more concentrated. This is probably the reason why strong acids and ammonia are underestimated in the model compared to the data, for low values of the liquid water content. The overestimation of aqueous formic acid could be explained by the high gaseous initial formaldehyde concentration that was assumed from another data set.

Table 12 presents estimations of deviations from Henry's law from the literature and from the study of Voisin et al. (2000) that are represented by the partitioning q factor, previously defined in Section 2.3. Calculated values from our work are compared to field measurements and to model results of Herrmann et al. (2000). First, a great variability is found in the various experimental studies. In the model results, most of the soluble species are at equilibrium with Henry's law, except nitric acid in our simulation which has a low q factor less than 1 and S(IV) which has a high factor q greater than 1. Formic acid, hydrochloric acid and ammonia are not very reactive either in gas phase or aqueous phase while nitric acid is very efficiently produced (with a speed of gaseous production faster than its speed of transfer towards aqueous phase) in gas phase in our case with high

NO_x levels. Discrepancies between observations and model results can be explained by the limitations already mentioned in the model which does not account for microphysical and dynamical processes, probably responsible of observed deviations from Henry's law. However, our results are in good agreement with simulated results by Herrmann et al. (2000).

3.4. Sensitivity to drop sizes

As already pointed out, measurements of droplets radius were not available on December 13th, 1997. So, we have performed a sensitivity test on the droplet radius for three values: 1, 10 and 100 μm and in the same conditions described in Tables 10 and 11 and in Fig. 2. The droplet surface is larger for 1 μm and the concentrations of species in aqueous phase are greater than for 10 μm and 100 μm . We choose to look into more details to the sensitivity of the gas-phase production of HO_2 radical to droplet radius. In fact, this radical is soluble (cf. Tables 1 and 2) and its scavenging perturbs the gas-phase ozone formation and leads to a HO_x -catalyzed cycle for the destruction of O_3 in aqueous phase (Lelievre and Crutzen, 1991). Fig. 4 shows the gas-phase production rates of HO_2 radical at the maximum of the liquid water content (0.22 g m^{-3}) at 1.22 p.m. local time for the three values of the droplet radius. For 1 μm , an important production of the HO_2 radical due to degassing of the droplet occurs (through transfer). It is associated to an important aqueous-phase production of the HO_2 radical due to the oxidation of formaldehyde and formic acid by the hydroxyl radical. The main gas-phase production pathway of HO_2 from the photolysis of formaldehyde and the oxidation of CO by OH increases with the droplet radius. However, the total production is minimum for 10 μm because the aqueous-phase production from the oxidation of formaldehyde and formic acid is faster than the gas-phase production from the oxidation of formaldehyde and carbon monoxide. This example on the gas-phase production of the HO_2 radical shows an important sensitivity to the droplet radius and highlights the high reactivity of the aqueous phase versus the gas-phase.

4. Cloud chemistry during the event

In this section, model results will be analyzed and chemical regimes will be compared to the theoretical work of Herrmann et al. (2000), which includes more species (transition metals and C2 chemistry) but neglects some pathways such as OHCH_2O_2 reactivity. Also, in case of Herrmann's (2000) the liquid water content is held constant throughout the simulation and the droplet radius is much smaller (1 μm instead of 10 μm in this work).

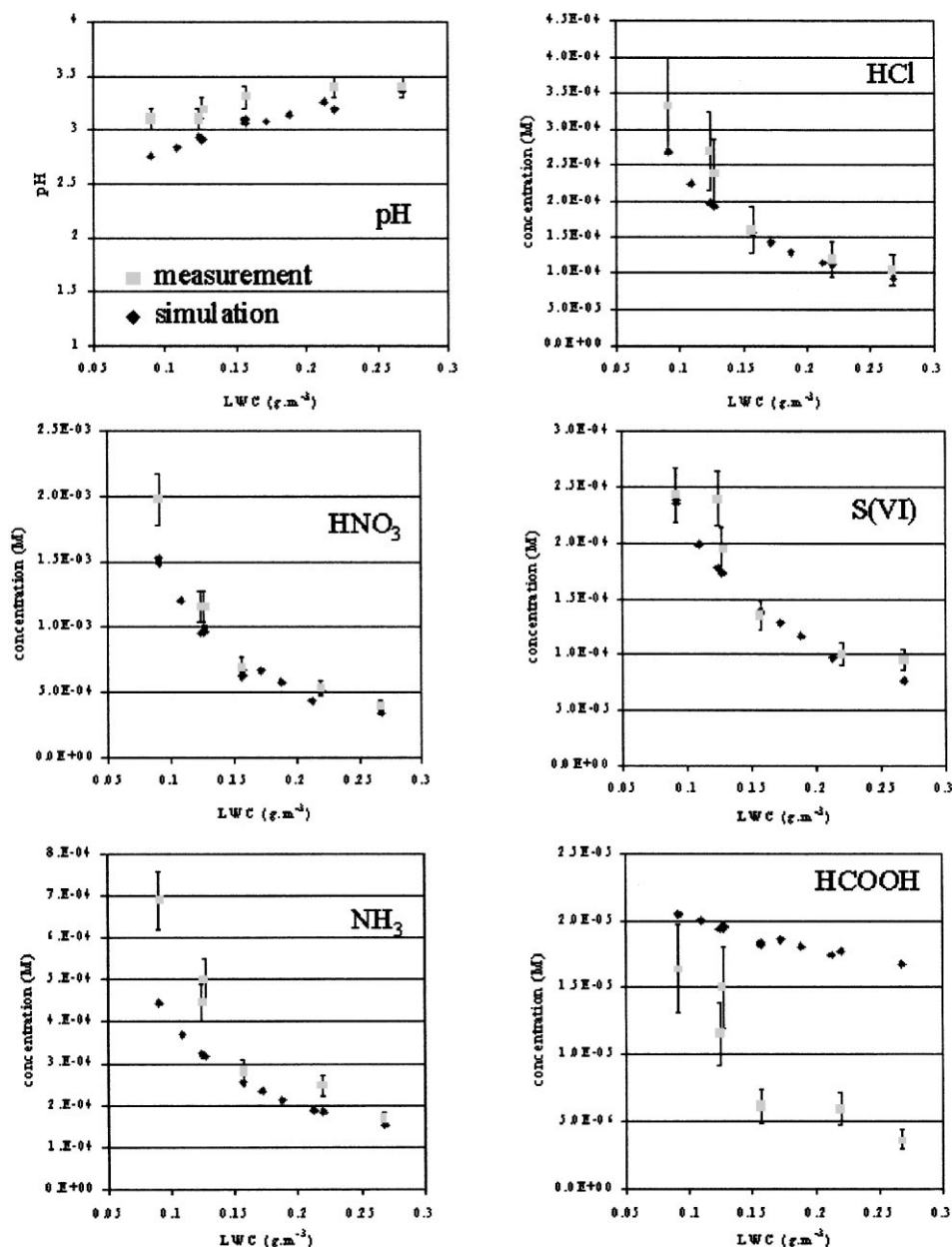


Fig. 3. Comparison of aqueous concentration and pH measured and simulated for different values of liquid water content. Error bars are reported for the aqueous phase measurements.

4.1. Radical chemistry

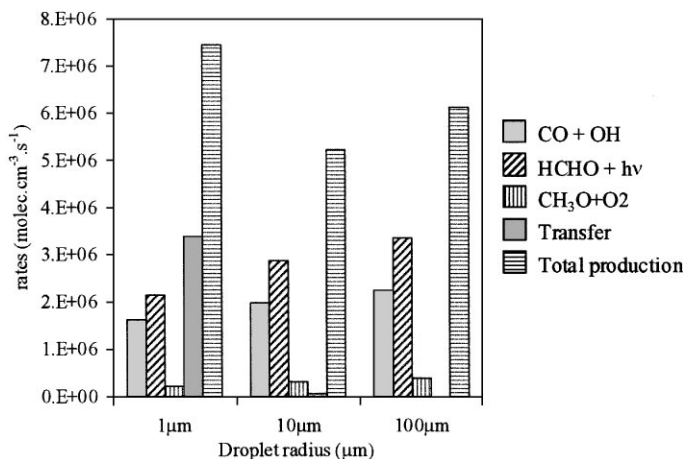
Radicals are very reactive species, responsible for the oxidizing capacity of the atmosphere. OH is the most important radical both in gas phase and aqueous phase. The sources of OH radical in aqueous phase is mainly transfer from the gas phase (60%), followed by the OH_{aq} production by ozone reaction with the superoxide ion (25%) and by nitrate ion photolysis (15%). Sinks for the

OH_{aq} radical are due to the oxidation of the hydrated formaldehyde by OH (80%), leaving behind minor contributions of others reactions like A12 in Table 4 and A111 and A112 in Table 7. In our scenario, a mean gas-phase concentration of $2 \times 10^6 \text{ molec cm}^{-3}$ and a mean aqueous-phase concentration of about $2 \times 10^{-14} \text{ M}$ are found whereas in Herrmann et al. (2000) larger values are obtained in aqueous phase, of the order of $2 \times 10^{-12} \text{ M}$. This can be explained by looking

Table 12

Estimations of deviations from Henry's law, taken from the literature and compared with this work

Species	q factor	pH range	Ref.
HCOOH	0.001–2	7–3	Facchini et al. (1992) ^a
	0.003–40	7–3	Winiwarter et al. (1994) ^a
	0.01–10	7–3	Keene et al. (1995) ^a
	0.1–10	5.5–3	Laj et al. (1997) ^a
	0.01–1	5–3	Voisin et al. (2000) ^a
	1	2.7	Herrmann et al. (2000) ^b
HCl	1	3.4–2.7	This work
	10^{-8} – 10^{-4}	5–3	Voisin et al. (2000) ^a
HNO ₃	1	3.4–2.7	This work
	10^{-7} – 10^{-4}	5–3	Voisin et al. (2000) ^a
SIV	0.01–0.06	3.4–2.7	This work
	70–500	3.5–2	Richards et al. (1983) ^a
	0.001–10	7–3	Winiwarter et al. (1994) ^a
	0.1–10	5.5–3	Laj et al. (1997) ^a
	0.1–10	5–3	Voisin et al. (2000) ^a
NH ₃	11	2.7	Herrmann et al. (2000) ^b
	1–8	3.4–2.7	This work
	0.01–10	7–3	Facchini et al. (1992) ^a
	0.001–1	7–3	Winiwarter et al. (1994) ^a
	0.05–0.2	5–3	Voisin et al. (2000) ^a
	1	3.4–2.7	This work

^aDeduced from experimental studies.^bResults of Herrmann et al. model, (2000) after 36 h of simulation and calculated from values of the two partitioning coefficients ε and $\varepsilon_{\text{henry}}$ by the relationship: $q = (\varepsilon(1 - \varepsilon_{\text{henry}})/\varepsilon_{\text{henry}}(1 - \varepsilon))$, we can notice here that due to value of ε and $\varepsilon_{\text{henry}}$ equal to 1 for nitric acid, its q factor from the study of Herrmann et al. (2000) cannot be determined.Fig. 4. Rates of gas-phase production of the HO₂ radical at the maximum of the liquid water content (0.22 g m⁻³) at 1.22 p.m. local time for three values of the droplet radius.

at the reaction pathways leading to OH production in aqueous phase. There are several reasons for these discrepancies. First, in this study, the net transfer rate of OH in aqueous phase is two orders of magnitude lower than the one in Herrmann et al. (2000) and can be explained by the different values of the droplet radius and

of the liquid water content. As a result, the term: $Lk_i C_g^i$ in Herrmann et al. (2000) is larger than in our case. Since transition metal chemistry is not considered in this work, a source of OH in aqueous phase is neglected from the reaction between hydrogen peroxide and Fe²⁺/Cu⁺.

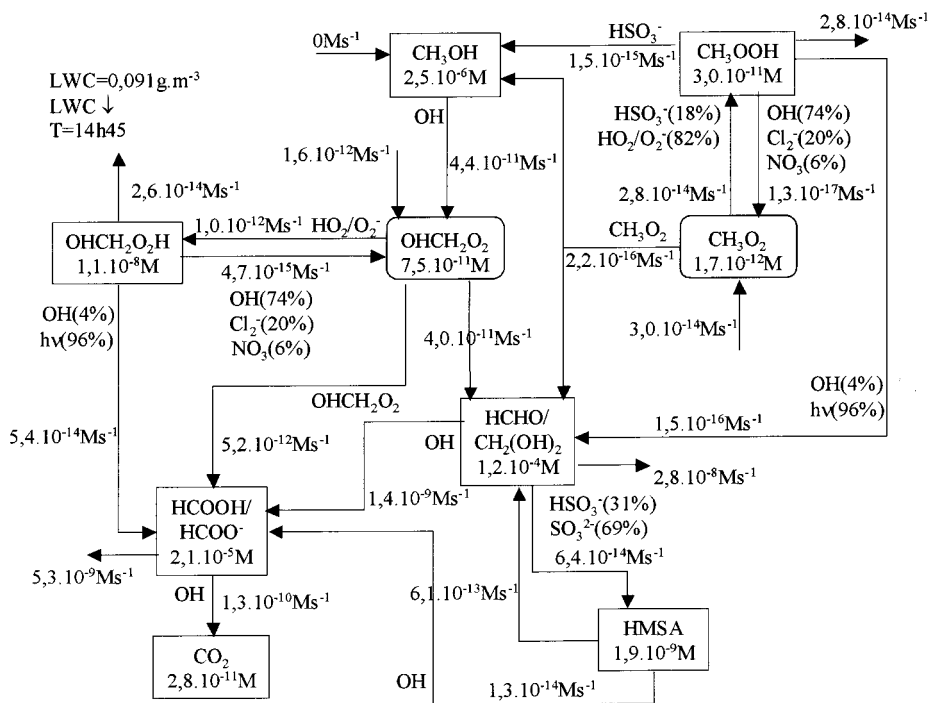


Fig. 6. Same as Fig. 5 but at 2.45 p.m. (=14h45) and at LWC = 0.091 g m⁻³.

source in aqueous phase from the oxidation of acetic acid of methyl peroxy CH_3O_2 radical. In Fig. 5, it is clearly seen that transfer from gas phase is the dominant source for volatile organic compounds, except for methyl hydroperoxide for which net aqueous-phase production in the droplets is faster than its gaseous production. This transfer operates as converting gaseous alcohols into aqueous formic acid and aldehydes that further oxidize into formic acid.

Fig. 6 is similar to Fig. 5, except that concentration/flux diagram is presented later on in the simulation. At this time, the liquid water content is smaller and is decreasing and gaseous material is less available than at the start of the simulation since the gas phase is not replenished by any dynamical or microphysical processes. Due to this difference, we observe a general decrease in the percentages of oxidation pathways of volatile organic compounds by radicals. Compared to the case where the cloud water content was increasing, we notice that hydrated formaldehyde is not anymore in equilibrium with hydroxymethanesulfonate (Reactions A120–A123 in Table 6) since there is less sulfite available to form HMSA. Also with decreasing liquid water content, all organic volatile compounds are degassing with negative transfer rates, contrasting with the situation previously observed in Fig. 5. When the cloud dissipates with a decrease of its liquid water content, droplets are more concentrated in aqueous phase.

Finally, even if volatile organic compounds concentrations are in the same order of magnitude as in Herrmann et al. (2000), we observe slightly smaller values directly related to the fact that larger droplets are considered in our model, leading to a reduced total droplet surface associated with a reduced droplet number concentration.

4.3. Conversion of S(IV) to S(VI)

At last, the conversion from S(IV) to sulfate is partly at the origin of the acidification of the cloud. The main path of oxidation of S(IV) into sulfate is through reaction with H_2O_2 at low pH and with O_3 at high pH (Graedel and Weschler, 1981). The importance of metal ions, as catalysers has also been stressed in the literature (Grgic et al., 1991). In Fig. 7, production pathways of sulfate are drawn and in our conditions peroxyoxynitric acid is the main oxidizing agent of S(IV) into S(VI). The only reference mentioning the possible importance of peroxyoxynitric acid is Amels et al. (1996). In order to explain such a phenomenon, a budget of gaseous peroxyoxynitric acid is detailed in Fig. 8. In clear air, this acid is in equilibrium with $\text{HO}_2 + \text{NO}_2$. With the presence of clouds, this equilibrium is disrupted because of the high solubility of peroxyoxynitric acid. As can be seen in Fig. 8, the non-equilibrium is represented in the net gas reactivity production. Due to the net transfer destruction (Fig. 8), the

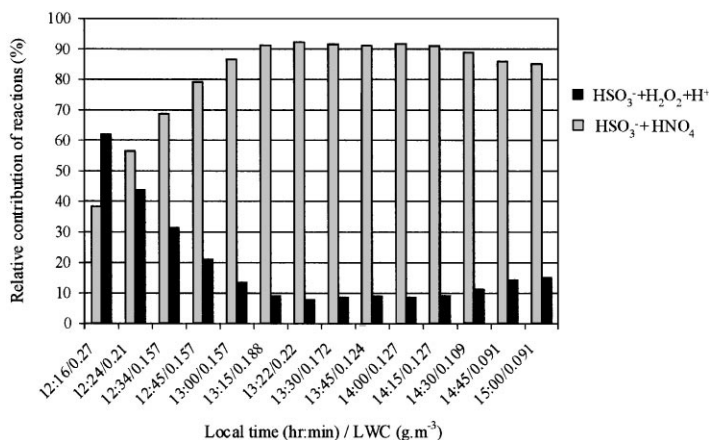


Fig. 7. Production pathways for sulfate at different time and liquid water content during the simulation.

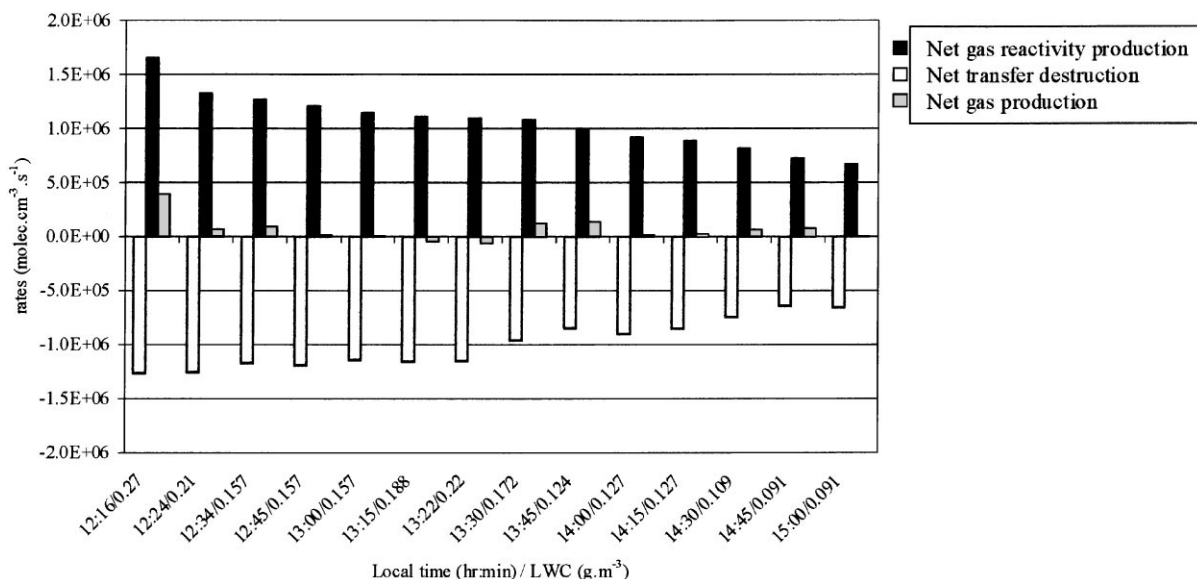


Fig. 8. Source and sink of peroxyoxynitric acid in gas phase for different time and liquid water content during simulation.

fraction that enters the aqueous phase is very significant to oxidize S(IV), especially in the present conditions of low H₂O₂ concentrations, increased by the fact that H₂O₂ is not refilled by any entrainment or other process that will renew its gas-phase concentration. In order to support such an hypothesis, a sensitivity test has been performed with initializing the chemical model with 1 ppb of H₂O₂. Results are shown in Fig. 9. Again, oxidation pathways of S(IV) into S(VI) are examined and we retrieve more classical conclusions. H₂O₂ is the main oxidant, but is closely followed by the peroxyoxynitric acid to a less extent in connection with high NO_x levels. At the end of the simulation, this time, other oxidation pathways appear with the reactions of Cl⁻ and H₂O₂

with the sulfate radical anion, due to the artifact of the box model that neglects cloud entrainment of fresh H₂O₂ oxidant.

The high NO_x regime that was observed during the CIME experiment, leading to a low hydrogen peroxide concentration, combined with unrealistic dynamical conditions in the chemical box model highlight the possible contribution of very soluble peroxyoxynitric acid in the conversion of S(IV) to S(VI).

Moreover, this result highlights the fact that peroxyoxynitric acid can contribute significantly to S(IV) to S(VI) conversion and can compete with H₂O₂ oxidation of S(IV) in aqueous phase and could partly explain degassing of H₂O₂ as observed by Laj et al. (1997).

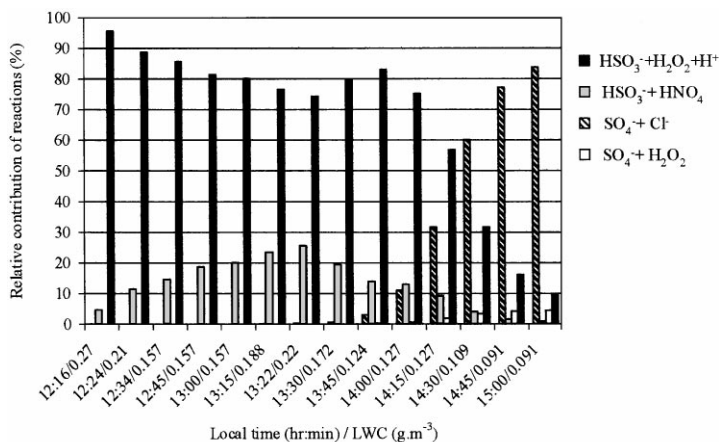


Fig. 9. Same as Fig. 7 but with an initial gas-phase concentration of hydrogen peroxide of 1 ppbv.

5. Conclusion

In this study, we have used a multiphase box model which takes into account an explicit chemistry mechanism for both gas and aqueous phase for a rural environment and the kinetic of mass transfer between phases (Schwartz, 1986). The model is, then, compared to multiphase measurements performed by Voisin et al. (2000) during the CIME experiment. The analysis of the evolutions in cloud droplets of key species with the liquid water content show that for the event of 13th December 1997, the cloud chemistry is mainly governed by high NO_x and high formaldehyde levels and by an acidic pH in the droplets. As an example, the gas-phase production of the HO_2 radical shows an important sensitivity to the droplet radius and highlights both the high reactivity of the aqueous phase versus the gas phase and the indirect effect of the liquid-phase reactivity on the gas species budget. Also, a comparison of the model results is performed versus recent theoretical results from Herrmann et al. (2000), who proposed a slightly different chemical scheme, including C2 chemistry and transition metal chemistry but neglecting some reaction pathways, such as the one involving OHCH_2O_2 radical and using different microphysical cloud conditions (cloud duration, constant liquid water content, small droplet radius).

On the basis of this double confrontation with observations and with theoretical results from Herrmann et al. (2000), a detailed analysis of radical chemistry and of the relative importance of those radicals in the oxidation of volatile organic compounds is performed. Depending on the stage of evolution of the cloud, either growing or dissipating, a different partitioning of organic volatile compounds is observed between the gas phase and the aqueous phase. Also, some equilibrium such as the

one between hydrated formaldehyde and hydroxymethanesulfonate are not valid anymore when varying the liquid water content.

Then, evidence for the possible role of aqueous peroxonitric acid in the conversion of S(IV) to S(VI), already underlined by Amels et al. (1996) has been found in case of low hydrogen peroxide concentration levels associated to the high NO_x regime observed during the experiment.

These results show the capability of such a chemical box model, including exhaustive and explicit multiphase chemistry of highlighting wild variability in reaction and oxidation pathways, that cannot be directly put in evidence through actual measurements. They also indicate the need for lacking observations of gases such as formaldehyde that would greatly help this kind of approach.

In conclusion, this study shows the difficulty to interpret multiphase measurements with a modeling tool in the actual state of knowledge. It also demonstrates that the set of measurements is incomplete and that there is a strong need for closer interactions between modelers and experimentalists. However, we anticipate that we should be able to improve the comparison between model and measurements by coupling the multiphase chemistry model with a microphysical model. Microphysical processes should introduce more dynamics in the model and should simulate a multiphase chemical system closer to the complex reality of natural clouds.

Acknowledgements

This work was supported by the “Programme National de Chimie Atmosphérique” (PNCA) of the INSU (Institut des Sciences de l’Univers). It was performed in close cooperation with the CIME project which was funded by the European Commission under

ENV4-CT95-0012. Computer resources were provided by I.D.R.I.S (Institut du développement et des Ressources en Informatiques Scientifique), project No. 000187.

References

- Amels, P., Elias, H., Götz, U., Steinges, U., Wannowius, K.J., 1996. Kinetic investigation of the stability of peroxonitric acid and of its reaction with sulfur(IV) in aqueous solution. In: Warneck, P. (Ed.), *Heterogeneous and Liquid Phase Processes, Transport and Chemical Transformation of Pollutants in the Troposphere*, Vol. 2. Springer, Berlin, pp. 77–88.
- Audiffren, N., Renard, M., Buisson, E., Chaumerliac, N., 1998. Deviations from the Henry's law equilibrium during cloud events: a numerical approach of the mass transfer between phases and specific numerical effects. *Atmospheric Research* 49 (2), 139–161.
- Aumont, B., Madronich, S., Bey, I., Tyndall, G.S., 1999. Contribution of secondary VOC to the composition of aqueous atmospheric particles: a modeling approach. *Journal of Atmospheric Chemistry* 35 (1), 59–75.
- Becker, K.H., Kleffmann, R., Kurtenbach, R., Wiesen, P., 1996. Solubility of nitrous acid (HONO) in sulfuric acid solutions. *Journal of Physical Chemistry* 100, 14984–14990.
- Bell, R.P., 1966. The reversible hydration of carbonyl compounds. *Advances in Physical Organic Chemistry* 4, 1–29.
- Betterton, E.A., Hoffmann, M.R., 1988a. Henry's law constants of some environmentally important aldehydes. *Environmental Science and Technology* 22, 1415–1418.
- Betterton, E.A., Hoffmann, M.R., 1988b. Oxidation of aqueous SO₂ by peroxymonosulfate. *Journal of Physical Chemistry* 92, 5962–5965.
- Bielski, B.H.H., 1978. Reevaluation of the spectral and kinetic properties of the HO₂ and O₂⁻ free radicals. *Photochemistry and Photobiology* 28, 645–649.
- Bjergbakke, E., Navaratnam, S., Parsons, B.J., Swallow, A.J., 1981. Reaction between HO₂ and chlorine in aqueous solution. *Journal of American Chemical Society* 103, 5926–5928.
- Bongartz, A., Kames, J., Schurath, U., George, Ch., Mirabel, Ph., Ponche, J.L., 1994. Experimental determination of HONO mass accommodation coefficients using two different techniques. *Journal of Atmospheric Chemistry* 18 (2), 149–170.
- Bongartz, A., Schweighofer, S., Roose, C., Schurath, U., 1995. The mass accommodation coefficient of ammonia on water. *Journal of Atmospheric Chemistry* 20 (1), 35–58.
- Bott, A., 1999. A numerical model of the cloud-topped planetary boundary-layer: chemistry in marine stratus and the effects on aerosol particles. *Atmospheric Environment* 33 (12), 1921–1936.
- Buxton, G.V., 1994. Mechanisms for chemical reactions in cloud droplets. In: Borrell, P.M., Borrell, P., Cvitas, T., Seiler, W. (Eds.), *Proceedings of EUROTRAC Symposium '94: Transport and Chemical Transformation of Pollutants in the Troposphere*. SPB Academic Publishing, The Hague, pp. 978–983.
- Buxton, G.V., Greenstock, C.L., Helman, N.P., Ross, H.B., 1988. Critical review of rate constants for reactions of hydrated electrons, hydrogen atoms and hydroxyl radicals in aqueous solution. *Journal of Physical Chemistry Reference Data* 17, 513–886.
- Buxton, G.V., Malone, T.N., Salmon, G.A., 1996a. A pulse radiolysis study of the reaction of SO₅⁻ with HO₂. In: Mirabel, Ph. (Ed.), *Air Pollution Research Report 57: Homogenous and Heterogeneous Chemical Processes in the Troposphere*. Office for Official Publications of the European Communities, Luxembourg, pp. 133–137.
- Buxton, G.V., McGowan, S., Salmon, G.A., Williams, J.E., Wood, N.D., 1996b. A study of the spectra and reactivity of oxysulphur radical anions involved in the chain oxidation of S(IV): a pulse and gamma-radiolysis study. *Atmospheric Environment* 30 (14), 2483–2493.
- Buxton, G.V., Salmon, G.A., Wood, N.D., 1990. A pulse radiolysis study of the chemistry of oxysulfur radicals in aqueous solution. In: Restelli, G., Angeletti, G. (Eds.), *Proceedings of the Fifth European Symposium: Physico-Chemical Behavior of Atmospheric Pollutants*. Kluwer, Dordrecht, pp. 245–250.
- Chaumerliac, N., Leriche, M., Audiffren, N., 2000. Modelling of chemical processes in clouds: scavenging and partitioning of species among gas and liquid phases. *Atmospheric Research* 53 (1-3), 29–43.
- Chin, M., Wine, P.H., 1994. A temperature-dependent competitive kinetics study of the aqueous-phase reactions of OH radicals with formate, formic acid, acetate, acetic acid, and hydrated formaldehyde. In: Helz, G.R., Zepp, R.G., Crosby, D.G. (Eds.), *Aquatic and Surface Photochemistry*. CRC Press, Boca Raton, pp. 85–98.
- Christensen, H., Sehested, K., Corfitzen, H., 1982. Reactions of hydroxyl radicals with hydrogen peroxide at ambient and elevated temperatures. *Journal of Physical Chemistry* 86, 1588–1590.
- Christensen, H., Sehested, K., 1988. HO₂ and O₂⁻ radicals at elevated temperatures. *Journal of Physical Chemistry* 92, 3007–3011.
- Clegg, S.L., Brimblecombe, P., 1989. Solubility of ammonia in pure aqueous and multicomponent solutions. *Journal of Physical Chemistry* 93, 7237–7238.
- Clifton, C.L., Huie, R.E., 1989. Rate constants for hydrogen abstraction reactions of the sulfate radical, SO₄⁻. *Alcohols*. *International Journal of Chemical Kinetics* 21, 677–687.
- Clifton, C.L., Huie, R.E., 1993. Rate constants for some hydrogen abstraction reactions of the carbonate radical. *International Journal of Chemical Kinetics* 25, 199–203.
- Collett Jr., J.L., Daube Jr., B.C., Gunz, D., Hoffmann, M.R., 1990. Intensive studies of Sierra Nevada cloudwater chemistry and its relationship to precursor aerosol and gas concentrations. *Atmospheric Environment* 24A (7), 1741–1757.
- Colville, R.N., Sander, R., Choularton, T.W., Bower, K.N., Inglis, D.W.F., Wobrock, W., Schell, D., Svenningsson, I.B., Wiedensohler, A., Hansson, H.-C., Hallberg, A., Ogren, J.A., Noone, K.J., Facchini, M.C., Fuzzi, S., Orsi, G., Arends, B.G., Winniwarter, W., Schneider, T., Berner, A., 1994. Computer modelling of clouds at Kleiner Feldberg. *Journal of Atmospheric Chemistry* 19, 189–229.
- Cotton, F.A., Wilkinson, G., 1967. *Advanced Inorganic Chemistry*, 2nd Edition. Wiley-Interscience, New York.
- Damschen, D.E., Martin, L.R., 1983. Aqueous aerosol oxidation of nitrous acid by O₂, O₃, and H₂O₂. *Atmospheric Environment* 17, 2005–2011.

- Daniels, M., 1968. Radiolysis and photolysis of the aqueous nitrate system. *Advances in Chemistry Series* 81, 153–163.
- Davidovits, M., Hu, J.H., Worsnop, D.R., Zahniser, M.S., Kolb, C.E., 1995. Entry of gas molecules into liquids. *Faraday Discussion* 100, 65–82.
- Deister, U., Neeb, R., Helas, G., Warneck, P., 1986. Temperature dependence of the equilibrium $\text{CH}_2(\text{OH})_2 + \text{HSO}_3^- = \text{CH}_2(\text{OH})\text{SO}_3^- + \text{H}_2\text{O}$ in aqueous solution. *Journal of Physical Chemistry* 90, 3213–3217.
- Draganic, Z.D., Negron-Mendoza, A., Sehested, K., Vujosevic, S.I., Navarro-Gonzales, R., Albarran-Sanchez, M.G., Draganic, I.G., 1991. Radiolysis of aqueous solution of ammonium bicarbonate over a large dose range. *Radiation Physics and Chemistry* 38, 317–321.
- Elliot, A.J., 1989. A pulse radiolysis study of the temperature dependence of reactions involving H, OH and e_{aq}^- in aqueous solution. *Radiation Physics and Chemistry* 34, 753–758.
- Elliot, A.J., McCracken, D.R., 1989. Effect of temperature on O-reactions and equilibria: a pulse radiolytic study. *Radiation Physics and Chemistry* 33, 69–74.
- Elliot, A.J., Buxton, G., 1992. Temperature dependence of the reactions $\text{OH} + \text{O}_2^-$ and $\text{OH} + \text{HO}_2$ in water up to 200°C. *Journal of the Chemical Society. Faraday Transactions* 88 (17), 2465–2470.
- Eriksen, T.E., Lind, J., Merenyi, G., 1985. On the acid-base equilibrium of the carbonate radical. *Radiation Physics and Chemistry* 26, 197–199.
- Exner, M., Herrmann, H., Zellner, R., 1992. Laser-based studies of reactions of the nitrate radical in aqueous solution. *Berichte der Bunsengesellschaft für Physikalische Chemie* 96 (3), 470–477.
- Exner, M., Herrmann, H., Michel, J.W., Zellner, R., 1993. Laser pulse initiated measurements of NO_3 reactions with S(IV) and organic compounds in aqueous solutions. In: Borrell, P.M., Borrell, P., Cvitas, T., Seiler, W. (Eds.), *Proceedings of EUROTRAC Symposium '92: Photo-oxidants: Precursors and Products*. SPB Academic Publishing, The Hague, pp. 615–618.
- Exner, M., Herrmann, H., Zellner, R., 1994. Rate constants for the reactions of the NO_3 radical with $\text{HCOOH}/\text{HCOO}^-$ and $\text{CH}_3\text{COOH}/\text{CH}_3\text{COO}^-$ in aqueous solution between 278 and 328 K. *Journal of Atmospheric Chemistry* 18 (4), 359–378.
- Facchini, M.C.M., Fuzzi, S., Kessel, M., Wobrock, W., Jaeschke, W., Arends, B.G., Möls, J.J., Berner, A., Solly, I., Krusiz, C., Reischl, G., Pahl, S., Hallberg, A., Ogren, J.A., Fierlinger-Oberlininger, H., Marzorati, A., Schell, D., 1992. The chemistry of sulfur and nitrogen species in a fog system. A multiphase approach. *Tellus* 44B (5), 505–521.
- Fried, A., Henry, B.E., Calvert, J.G., Mozurkewich, M., 1994. The reaction probability of N_2O_5 with sulfuric acid aerosols at stratospheric temperatures and composition. *Journal of Geophysical Research* 99D, 3517–3532.
- Gear, C.W., 1971. *Numerical Initial Value Problems in Ordinary Differential Equation*. Prentice-Hall, Englewood Cliffs, NJ, pp. 158–166.
- George, C., Ponche, J.L., Mirabel, Ph., Behnke, W., Scheer, V., Zetzsch, C., 1994. Study of uptake of N_2O_5 by water and NaCl solutions. *Journal of Physical Chemistry* 98 (35), 8780–8784.
- Geremy, G., Wobrock, W., Flossmann, A.I., Schwarzenbröck, A., Mertes, S., 2000. A modelling study on the activation of small aiten-mode aerosol particles during CIME 97. *Tellus* 52B (3), 959–979.
- Graedel, T.E., Goldberg, K.I., 1983. Kinetic studies of raindrop chemistry, 1, inorganic and organic processes. *Journal of Geophysical Research* 88, 10865–10882.
- Graedel, T.E., Weschler, C.J., 1981. Chemistry within aqueous atmospheric aerosols and raindrops. *Reviews of Geophysics and Space Physics* 19 (4), 505–539.
- Grégoire, P.J., Chaumerliac, N., Nickerson, E.C., 1994. Impact of cloud dynamics on tropospheric chemistry: advances in modelling the interactions between microphysical and chemical processes. *Journal of Atmospheric Chemistry* 18 (3), 247–266.
- Grgic, I., Hudnik, V., Bizjak, M., Levect, J., 1991. Aqueous S(IV) oxidation I. Catalytic effects of some metal ions. *Atmospheric Environment* 25A, 1591–1597.
- Hanson, D.R., Burkholder, J.B., Howard, C.J., Ravishankara, A.R., 1992. Measurements of OH and HO_2 radical uptake coefficients on water and sulfuric acid surfaces. *Journal of Physical Chemistry* 96, 4979–4985.
- Herrmann, H., Ervens, B., Nowacki, P., Wolke, R., Zellner, R., 1999a. A chemical aqueous phase radical mechanism for tropospheric chemistry. *Chemosphere* 38 (6), 1223–1232.
- Herrmann, H., Ervens, B., Jacobi, H.-W., Wolke, R., Nowacki, P., Zellner, R., 2000. CAPRAM2.3: a chemical aqueous phase radical mechanism for tropospheric chemistry. *Journal of Atmospheric Chemistry* 36 (3), 231–284.
- Herrmann, H., Exner, M., Zellner, R., 1994. Reactivity trends in reactions of the nitrate radical (NO_3) with inorganic and organic cloudwater constituents. *Geochimica et Cosmochimica Acta* 58 (15), 3239–3244.
- Herrmann, H., Jacobi, H.-W., Zellner, R., 1997. Laboratory studies of small radicals and radical anions of interest for tropospheric aqueous phase chemistry: the reactivity of SO_x^- . In: Borrell, P.M., Borrell, P., Cvitas, T., Kelly, K., Seiler, W. (Eds.), *Proceedings of EUROTRAC Symposium '96: Transport and Chemical Transformation of Pollutants in the Troposphere, Vol. 1. Computational Mechanics Publications, Southampton*, pp. 407–411.
- Herrmann, H., Reese, A., Ervens, B., Wicktor, F., Zellner, R., 1999b. Laboratory and modelling studies of tropospheric multiphase conversions involving some C1 and C2 peroxy radicals. *Physics and Chemistry of the Earth – Part B* 24 (3), 287–290.
- Herrmann, H., Zellner, R., Reese, A., 1995. Time-resolved UV/VIS diode array absorption spectroscopy of SO_x^- ($x = 3, 4, 5$) radical anions in aqueous solution. *Journal of Molecular Structure* 348, 183–186.
- Hewitt, C.N., Kok, G.L., 1991. Formation and occurrence of organic hydroperoxides in the troposphere: laboratory and field observations. *Journal of Atmospheric Chemistry* 12, 181–194.
- Hoffmann, M.R., 1986. On the kinetics and mechanism of oxidation of aequated sulfur dioxide by ozone. *Atmospheric Environment* 20, 1145–1154.
- Hoffmann, M.R., Calvert, J.G., 1985. Chemical transformation modules for Eulerian acid deposition models, Vol. 2, The aqueous-phase chemistry. Report EPA/600/3-85/017, Environmental Protection Agency, Research Triangle Park, N.C.

- Huie, R.E., Clifton, C.L., 1990. Temperature dependence of the rate constants for reactions of the sulfate radical, SO_4^- , with anions. *Journal of Physical Chemistry* 94 (23), 8561–8567.
- Huie, R.E., Shoute, L., Neta, P., 1991. Temperature dependence of the rate constants for reactions of the carbonate radical with organic and inorganic reductants. *International Journal of Chemical Kinetics* 23, 541–542.
- Huie, R.E., Clifton, C.L., 1993. Kinetics of the self-reaction of hydroxymethylperoxyl radicals. *Chemical Physics Letters* 205(2)(3), 163–167.
- Huret, N., Chaumerliac, N., Isaka, H., Nickerson, E.C., 1994. Influence of different microphysical schemes on the prediction of dissolution of nonreactive gases by cloud droplets and raindrops. *Journal of Applied Meteorology* 33 (9), 1096–1109.
- Jacob, D.J., 1986. Chemistry of OH in remote clouds and its role in the production of formic acid and peroxymonosulfate. *Journal of Geophysical Research* 91 (D9), 9807–9826.
- Jacobi, H.-W., 1996. Kinetische Untersuchungen und Modellrechnungen zur troposphärischen Chemie von Radikalanionen und Ozon in wässriger Phase, Ph.D. Thesis, University-GH-Essen, Germany.
- Jacobi, H.-W., Herrmann, H., Zellner, R., 1996. Kinetic investigation of the Cl_2^- radical in the aqueous phase. In: Mirabel, Ph. (Ed.), *Air Pollution Research Report 57: Homogenous and Heterogeneous Chemical Processes in the Troposphere*. Office for Official Publications of the European Communities, Luxembourg, pp. 172–176.
- Jacobi, H.-W., Herrmann, H., Zellner, R., 1997. A laser flash photolysis study of the decay of Cl-atoms and Cl_2^- radical anions in aqueous solution at 298 K. *Berichte der Bunsengesellschaft für Physikalische Chemie* 101 (12), 1909–1913.
- Jacobi, H.-W., Wicktor, F., Herrmann, H., Zellner, R., 1999. A laser flash photolysis kinetic study of reactions of the Cl_2^- radical anion with oxygenated hydrocarbons in aqueous solution. *International Journal of Chemical Kinetics* 31 (3), 169–181.
- Jaeschke, W., Dierssen, J.P., Günther, A., Schumann, M., 1998. Phase partitioning of ammonia and ammonium in a multiphase system studied using a new vertical wet denuder technique. *Atmospheric Environment* 32 (3), 365–371.
- Jayne, J.T., Duan, S.X., Davidovits, P., Worsnop, D.R., Zahniser, M.S., Kolb, C.E., 1991. Uptake of gas-phase alcohol and organic acid molecules by water surfaces. *Journal of Physical Chemistry* 95, 6329–6336.
- Jayson, G.G., Parson, B.J., Swallow, A.J., 1973. Some simple, highly reactive, inorganic chlorine derivatives in aqueous solution. *Journal of Chemical Society Faraday Transactions* 69, 1597–1607.
- Jiang, P.-Y., Katsumura, Y., Nagaishi, R., Domae, M., Ishikawa, K., Ishigure, K., Yoshida, Y., 1992. Pulse radiolysis study of concentrated sulfuric acid solutions. *Journal of the Chemical Society Faraday Transactions* 88, 1653–1658.
- Johnson, B.J., Betterton, E.A., Craig, D., 1996. Henry's law coefficients of formic and acetic acids. *Journal of Atmospheric Chemistry* 24, 113–119.
- Kames, J., Schurath, U., 1992. Alkyl nitrates and bifunctional nitrates of atmospheric interest: Henry's law constant and their temperature dependencies. *Journal of Atmospheric Chemistry* 15, 79–95.
- Keene, W.C., Mosher, B.W., Jacob, D.J., Munger, J.W., Talbot, R.W., Artz, R.S., Maben, J.R., Daube, B.C., Galloway, J.N., 1995. Carboxylic acids in clouds at a high-elevation forested site in central Virginia. *Journal of Geophysical Research* 100 (D5), 9345–9357.
- Kieber, R.J., Rhines, M.F., Willey, J.D., Brooks Avery Jr., G., 1999. Rainwater formaldehyde: concentration, deposition and photochemical formation. *Atmospheric Environment* 33 (22), 3659–3667.
- Kosak-Channing, L.F., Helz, G.R., 1983. Solubility of ozone in aqueous solutions of 0–0.6 M ionic strength at 5–30°C. *Environmental Science and Technology* 17, 145–149.
- Laj, P., Fuzzi, S., Facchini, M.C., Lind, J.A., Orsi, G., Preiss, M., Maser, R., Jaeschke, W., Seyffer, E., Helas, G., Acker, K., Wiprecht, W., Möller, D., Arends, B.G., Möls, J.J., Colvile, R.N., Gallagher, M.W., Beswick, K.M., Hargreaves, K.J., Storeron-West, R.L., Sutton, M.A., 1997. Cloud processing of soluble gases. *Atmospheric Environment* 31 (16), 2589–2598.
- Lammel, G., Perner, D., Warneck, P., 1990. Decomposition of pernitric acid in aqueous solution. *Journal of Physical Chemistry* 94, 6141–6144.
- Lee, Y.-N., Lind, J.A., 1986. Kinetics of aqueous oxidation of nitrogen(III) by hydrogen peroxide. *Journal of Geophysical Research* 91, 2793–2800.
- Leibrock, E., Slemr, J., 1997. Method for measurements of volatile oxygenated hydrocarbons in ambient air. *Atmospheric Environment* 31 (20), 3329–3339.
- Lelieveld, J., Crutzen, P.J., 1991. The role of clouds in tropospheric photochemistry. *Journal of Atmospheric Chemistry* 12, 227–229.
- Lide, D.R., Frederikse, H.P.R., 1995. *Handbook of Chemistry and Physics*, 76th Edition. CRC Press, Inc., Boca Raton, FL.
- Lind, J.A., Lazrus, A.L., Kok, G.L., 1987. Aqueous phase oxidation of sulfur(IV) by hydrogen peroxide, methylhydroperoxide, and peroxyacetic acid. *Journal of Geophysical Research* 92 (D4), 4171–4177.
- Logager, T., Sehested, K., 1993. Formation and decay of peroxyntic acid: a pulse radiolysis study. *Journal of Physical Chemistry* 97, 10047–10052.
- Logager, T., Sehested, K., Holoman, J., 1993. Rate constants of the equilibrium reactions $\text{SO}_4^- + \text{HNO}_3 \rightleftharpoons \text{HSO}_4^- + \text{NO}_3$ and $\text{SO}_4^- + \text{NO}_3^- \rightleftharpoons \text{SO}_4^{2-} + \text{NO}_3$. *Radiation Physics and Chemistry* 41, 539–543.
- Long, C.A., Bielski, B.H.J., 1980. Rate of reaction of superoxide radical with chloride-containing species. *Journal of Physical Chemistry* 84, 555–557.
- Losno, R., Colin, J.L., Spokes, L., Jickells, T., Schulz, M., Rebers, A., Leermakers, M., Meuleman, C., Baeyens, W., 1998. Non-rain deposition significantly modifies rain samples at a coastal site. *Atmospheric Environment* 32 (20), 3445–3455.
- Maaß, F., Elias, H., Wannowius, K.J., 1999. Kinetics of oxidation of hydrogen sulfite by hydrogen peroxide in aqueous solution: ionic strength effects and temperature dependence. *Atmospheric Environment* 33 (27), 4413–4419.
- Madronich, S., 1987. Photodissociation in the atmosphere. *Journal of Geophysical Research* 92, 9740–9752.
- Madronich, S., Calvert, J.G., 1990. The NCAR Master Mechanism of the gas phase chemistry. NCAR Technical Note, TN-333 + SRT, Boulder Colorado.
- Madronich, S., Flocke, S., 1999. The role of solar radiation in atmospheric chemistry. In: Boule, P. (Ed.), *Environmental Photochemistry*. Springer, Berlin, pp. 1–26.

- Magi, L., Pallares, C., George, Ch., Mirable, Ph., 1996. Uptake of ozone by aqueous solutions. In: Mirable, Ph. (Ed.), Air Pollution Research Report 57: Homogeneous and Heterogeneous Chemical Processes in the Troposphere. Office for Official Publications of the European Communities, Luxembourg, pp. 24–29.
- Marsh, A.R.W., McElroy, W.J., 1985. The dissociation constant and Henry's law constant of HCl in aqueous solution. *Atmospheric Environment* 19, 1075–1080.
- Maruthamuthu, P., Neta, P., 1977. Radiolytic chain decomposition of peroxomonophosphoric and peroxomonosulfuric acids. *Journal of Physical Chemistry* 81, 937–940.
- Mihelcic, D., Klemp, D., Müsgen, P., Pätz, H.W., Volz-Thomas, A., 1993. Simultaneous measurements of peroxy and nitrate radicals at Schauinsland. *Journal of Atmospheric Chemistry* 16, 313–335.
- Möller, D., Mauersberger, D., 1995. Aqueous phase chemical reaction system used in cloud chemistry modelling. In: Flossmann, A., Cvitas, T., Möller, D., Mauersberger, G. (Eds.), *Clouds: Models and Mechanisms*, EUROTRAC Special Publications. ISS Garmisch-Partenkirchen, Germany, pp. 77–93.
- Monod, A., Carlier, P., 1999. Impact of clouds on the tropospheric ozone budget: direct effect of multiphase photochemistry of soluble organic compounds. *Atmospheric Environment* 33 (27), 4431–4446.
- Monod, A., Chebbi, A., Durand-Jolibois, R., Carlier, P., 2000. Oxidation of methanol by hydroxyl radicals in aqueous solution under simulated cloud droplet conditions. *Atmospheric Environment* 34, 5283–5294.
- National Bureau of Standards, 1965. Selected values of chemical thermodynamic properties, 1. N.B.S. Technical Note 270(1), 124 pp.
- Noone, K.J., Charlson, R.J., Covert, D.S., Ogren, J.A., Heintzenberg, J., 1988. Design and calibration of a counterflow virtual impactor for sampling of atmospheric fog and cloud droplets. *Aerosol Science and Technology* 8, 235–244.
- Noone, K.J., Ogren, J.A., Birgitta Noone, K., Hallberg, A., Fuzzi, S., Lind, J.A., 1991. Measurements of the partitioning of hydrogen peroxide in a stratiform cloud. *Tellus* 43B, 280–290.
- Olson, T.M., Hoffmann, M.R., 1989. Hydroxyalkylsulfonate formation: its role as a S(IV) reservoir in atmospheric water droplets. *Atmospheric Environment* 23 (5), 985–997.
- O'Sullivan, D.W., Lee, M., Noone, B.C., Heikes, B.G., 1996. Henry's law constant determinations for hydrogen peroxide, methyl hydroperoxide, hydroxymethyl hydroperoxide, ethyl hydroperoxide, and peroxyacetic acid. *Journal of Physical Chemistry* 100, 3241–3247.
- Padmaja, S., Neta, P., Huie, R.E., 1993. Rate constant for some reactions of inorganic radicals with inorganic ions. Temperature dependence and solvent dependence. *Journal of Physical Chemistry* 25 (3), 445–455.
- Park, J.-Y., Lee, Y.-N., 1988. Solubility and decomposition kinetics of nitrous acid in aqueous solution. *Journal of Physical Chemistry* 92, 6294–6302.
- Ponche, J.L., George, Ch., Mirabel, Ph., 1993. Mass transfer at the air/water interface: mass accommodation coefficients of SO₂, HNO₃, NO₂ and NH₃. *Journal of Atmospheric Chemistry* 16 (1), 1–21.
- Pruppacher, H.R., Klett, J.D. (1997). *Microphysics of Clouds and Precipitation*, 2nd Edition. Reidel, Dordrecht, 954 pp.
- Richards, L.W., 1995. Airborne chemical measurements in nighttime stratus clouds in the Los Angeles basin. *Atmospheric Environment* 29 (1), 27–46.
- Richards, L.W., Anderson, J.A., Blumenthal, D.L., McDonald, J.A., 1983. Hydrogen peroxide and sulfur (IV) in Los Angeles cloud water. *Atmospheric Environment* 17 (4), 911–914.
- Ravishankara, A.R., 1997. Heterogeneous and multiphase chemistry in the troposphere. *Science* 276, 381–384.
- Redlich, O., 1946. The dissociation of strong electrolytes. *Chemical Review* 39, 333–356.
- Régimbal, J.-M., Mozurkewich, M., 1997. Peroxynitric acid decay mechanisms and kinetics at low pH. *Journal of Physical Chemistry A* 101, 8822–8829.
- Rettich, T.R., 1978. Some photochemical reactions of aqueous nitric acid. *Dissertation Abstracts International B. the Sciences and Engineering* 38, 59–68.
- Rudich, Y., Talukdar, R.K., Ravishankara, A.R., Fox, R.W., 1996. Reactive uptake of NO₃ on pure water and ionic solutions. *Journal of Geophysical Research* 101, 21023–21031.
- Ruggaber, A., Dlugi, R., Bott, A., Forkel, R., Hermann, H., Jacobi, H.-W., 1997. Modelling of radiation quantities and photolysis frequencies in the aqueous-phase in the troposphere. *Atmospheric Environment* 31 (19), 3137–3150.
- Saastad, O.W., Ellermann, T., Nielsen, C.J., 1993. On the adsorption of NO and NO₂ on cold H₂O/H₂SO₄ surfaces. *Geophysical Research Letters* 20 (12), 1191–1193.
- Schmidt, K.H., 1972. Electrical conductivity techniques for studying the kinetics of radiation induced chemical reactions in aqueous solution. *International Journal for Radiation Physics and Chemistry* 4, 439–468.
- Schurath, U., Bongartz, A., Kames, J., Wunderlich, C., Carstens, T., 1996. Laboratory determination of physico-chemical rate parameters pertinent to mass transfer into cloud and fog droplets. In: Warneck, P. (Ed.), *Heterogeneous and Liquid Phase Processes, Transport and Chemical Transformation of Pollutants in the Troposphere*, Vol. 2. Springer, Berlin, pp. 182–189.
- Schwartz, S.E., White, W.H., 1981. Solubility equilibria of the nitrogen oxides and oxiacids in dilute aqueous solution. *Advances in Environmental Science and Engineering* 4, 1–45.
- Schwartz, S.E., 1986. Mass-transport considerations pertinent to aqueous phase reactions of gases in liquid water clouds. In: Jaeschke, W. (Ed.), *Chemistry of Multiphase Atmospheric Systems*, NATO ASI Series, Vol. G6. Springer, Berlin, pp. 415–472.
- Sehested, K., Holeman, J., Hart, J.E., 1983. Rate constants and products of the reactions of e_{aq}⁻, O₂⁻ and H with ozone in aqueous solutions. *Journal of Physical Chemistry* 87, 1951–1954.
- Sehested, K., Holeman, J., Bjergbakke, E., Hart, E.J., 1984. A pulse radiolytic study of the reaction OH + O₃ in aqueous medium. *Journal of Physical Chemistry* 88, 4144–4147.
- Sehested, K., Logager, T., Holoman, J., Nielsen, O.J., 1994. Formation and reactions of the NO₃ radical in aqueous solution. In: Borrell, P.M., Borrell, P., Cvitas, T., Seiler, W. (Eds.), *Proceedings of EUROTRAC Symposium '94: Transport and Chemical Transformation of Pollutants in the Troposphere*. SPB Academic Publishing, The Hague, pp. 999–1004.

- Sillen, G.L., Martell, A.E., 1964. Stability constants of metal-ion complexes. Special Publication – Chemical Society 17, 357.
- Sillman, S., Logan, J.A., Wofsy, S.C., 1990. The sensitivity of ozone to nitrogen oxides and hydrocarbons in regional ozone episodes. *Journal of Geophysical Research* 95, 1837–1851.
- Smith, B.T., 1967. ZERPOL: a zero finding algorithm for polynomials using Laguerre's method. Technical Report, Department of Computer Science. University of Toronto, Canada.
- Smith, R.M., Martell, A.E., 1976. *Critical Stability Constants, Vol. 4: Inorganic Complexes*. Plenum Press, New York.
- Snider, J.R., Dawson, G.A., 1985. Tropospheric light alcohols, carbonyls and acetonitrile: concentrations in the southwestern United States and Henry's law data. *Journal of Geophysical Research* 90 (D2), 3797–3805.
- Strehlow, H., Wagner, I., 1982. Flash photolysis in aqueous nitrite solutions. *Zeitschrift für Physikalisch Chemie (Wiesbaden)* 132, 151–160.
- Suzuki, T., Ohtaguchi, K., Koide, K., 1992. Application of principal components analysis to calculate Henry's law constant from molecular structure. *Computers and Chemistry* 16 (1), 41–52.
- Tang, Y., Thorn, R.P., Mauldin III, R.L., Wine, P.H., 1988. Kinetics and spectroscopy of the SO_4^- radical in aqueous solution. *Journal of Photochemistry and Photobiology A. Chemistry* 44, 243–258.
- Treinin, A., 1970. The photochemistry of oxyanions. *Israel Journal of Chemistry* 8, 103–113.
- Voisin, D., Legrand, A., Chaumerliac, N., 2000. Investigations of the scavenging of acidic gases and ammonia in mixed liquid solid water clouds at the Puy de Dôme mountain (France). *Journal of Geophysical Research* 105 (D5), 6817–6836.
- Wagner, I., Strehlow, H., Busse, G., 1980. Flash photolysis of nitrate ions in aqueous solution. *Zeitschrift für Physikalisch Chemie (Wiesbaden)* 123, 1–33.
- Wang, T.X., Margerum, D.W., 1994. Kinetics of reversible chlorine hydrolysis: temperature dependence and general-acid/base-assisted mechanisms. *Inorganic Chemistry* 33 (6), 1050–1055.
- Wells, M., Bower, K.N., Choularton, T.W., Cape, J.N., Sutton, M.A., Storeton-West, R.L., Fowler, D., Wiedensohler, A., Hansson, H.-C., Svenningsson, B., Swietlicki, E., Wendisch, M., Jones, B., Dollard, G., Acker, K., Wieprecht, W., Preiss, M., Arends, B.G., Pahl, S., Berner, A., Kruijs, C., Laj, P., Facchini, M.C., Fuzzi, S., 1997. The reduced nitrogen budget of an orographic cloud. *Atmospheric Environment* 31, 2599–2614.
- Wilkinson, J.H., 1965. *The Algebraic Eigenvalue Problem*. Clarendon Press, Oxford.
- Wine, P.H., Tang, Y., Thorn, R.P., Wells, J.R., Davis, D.D., 1989. Kinetics of aqueous-phase reactions of the SO_4^- radical with potential importance in cloud chemistry. *Journal of Geophysical Research* (94), 1085–1094.
- Winiwarter, W., Fierlinger, H., Puxbaum, H., Facchini, M.C., Arends, B.G., Fuzzi, S., Schell, D., Kaminski, U., Pahl, S., Schneider, T., Berner, A., Solly, I., Kruijs, C., 1994. Henry's law and the behavior of weak acids and bases in fog and cloud. *Journal of Atmospheric Chemistry* 19, 173–188.
- Worsnop, D.R., Zahniser, M.S., Kolb, C.E., Gardner, J.A., Watson, L.R., Van Doren, J.M., Jayne, J.T., Davidovits, P., 1989. Temperature dependence of mass accommodation of SO_2 and H_2O_2 on aqueous surfaces. *Journal of Physical Chemistry* 93, 1159–1172.
- Zellner, R., Exner, M., Herrmann, H., 1990. Absolute OH quantum yields in the laser photolysis of nitrate, nitrite and dissolved H_2O_2 at 308 and 351 nm in the temperature range 278–353 K. *Journal of Atmospheric Chemistry* 10, 411–425.
- Zellner, R., Herrmann, H., Exner, M., Jacobi, H.-W., Raabe, G., Reese, A., 1996. Formation and reactions of oxidants in the aqueous phase. In: Warneck, P. (Ed.), *Heterogeneous and Liquid Phase Processes, Transport and Chemical Transformation of Pollutants in the Troposphere*, Vol. 2. Springer, Berlin, pp. 146–152.
- Zheng, D.-Q., Gua, T.-M., Knapp, H., 1997. Experimental and modeling studies on the solubility of CO_2 , CHClF_2 , CHF_3 , $\text{C}_2\text{H}_2\text{F}_4$ and $\text{C}_2\text{H}_4\text{F}_2$ in water and aqueous NaCl solutions under low pressures. *Fluid Phase Equilibrium* 129, 197–209.